Title: The metabolic acclimation of *Arabidopsis thaliana* to arsenate is sensitized by the loss of mitochondrial LIPOAMIDE DEHYDROGENASE2, a key enzyme in oxidative metabolism.

Running Title: sensitivity of arsenate-dependent metabolism

Weihua Chen[1,2*], Nicolas L. Taylor[3,4], Yingjun Chi[1,2,5], A. Harvey Millar[3,4], Hans Lambers[1,2], Patrick M. Finnegan[1,2]

[1]School of Plant Biology, [2]Institute of Agriculture, [3]Australian Research Council Centre of Excellence in Plant Energy Biology, [4]Centre for Comparative Analysis of Biomolecular Networks, The University of Western Australia, Crawley (Perth), WA 6009, Australia and [5]National Key Laboratory of Crop Genetics and Germplasm Enhancement, National Center for Soybean Improvement, Nanjing Agricultural University, Nanjing 210095, China

[*]Present address: Research School of Biology, College of Medicine, Biology and Environment, Australian National University, Canberra, Australian Capital Territory 0200, Australia.

Corresponding author:

Patrick M. Finnegan

School of Plant Biology M084

Faculty of Science

The University of Western Australia

35 Stirling Highway, Crawley (Perth) 6009, Australia.

Telephone: +61 8 6488 8546

Fax: +61 8 6488 1108

Email: patrick.finnegan@uwa.edu.au

ABSTRACT

Mitochondrial LIPOAMIDE DEHYDROGENASE is essential for the activity of four mitochondrial enzyme complexes central to oxidative metabolism. The reduction in protein amount and enzyme activity caused by disruption of *mitochondrial LIPOAMIDE DEHYDROGENASE2* enhanced the arsenic sensitivity of *Arabidopsis thaliana*. Both arsenate and arsenite inhibited root elongation, decreased seedling size and increased anthocyanin production more profoundly in knock-out mutants than in wild-type seedlings. Arsenate also stimulated lateral root formation in the mutants. The activity of mitochondrial LIPOAMIDE DEHYDROGENASE in isolated mitochondria was sensitive to arsenite, but not arsenate, indicating that arsenite could be the mediator of the observed phenotypes. Steady-state metabolite abundances were only mildly affected by mutation of *mitochondrial LIPOAMIDE DEHYDROGENASE2*. In contrast, arsenate induced the remodelling of metabolite pools associated with oxidative metabolism in wild-type seedlings, an effect that was enhanced in the mutant, especially around the enzyme complexes containing mitochondrial LIPOAMIDE DEHYDROGENASE. These results indicate that mitochondrial LIPOAMIDE DEHYDROGENASE is an important protein for determining the sensitivity of oxidative metabolism to arsenate in *Arabidopsis*.

Keyword Index: mitochondrial metabolism, stress response, pyruvate dehydrogenase, 2-oxoglutarate dehydrogenase, glycine decarboxylase

INTRODUCTION

Arsenic (As) is commonly present in the environment, and is both a toxin and carcinogen (ICAR 2004). Exposure to elevated levels of As by consuming contaminated water or food poses a great health concern to tens of millions of people (Nordstrom 2002; Ahmed et al. 2006; Zhu, Williams & Meharg 2008). The predominant form of inorganic As in oxidising environments is arsenate [As(V)], while in reducing environments arsenite [As(III)] predominates. Being an analogue of phosphate, As(V) is taken up into plant cells via phosphate transporters (Meharg & Macnair 1990; Shin et al. 2004; Catarecha et al. 2007). Once in the cell, it can target phosphate-dependent processes (Rosen, Ajees & McDermott 2011, Finnegan & Chen 2012). As(V) is also readily reduced to As(III) by arsenate reductase and other processes in plant cells (Zhao et al. 2009; Németi et al. 2010, Finnegan & Chen 2012). As(III) has a high affinity for thiol (-SH) groups. The binding of As(III) to proteins has the potential to alter their activities, with wide-ranging consequences, including inhibition of enzymatic functions and cellular processes (Hughes 2002; Bergquist et al. 2009). However, little is known of the plant processes that are most sensitive to As (Finnegan & Chen 2012).

We recently reported, through screening of an activation-tagged *Arabidopsis thaliana* population, that As(V)-sensitive mutants arose from disruption of *plastidial LIPOAMIDE DEHYDROGENASE1 (ptLPD1)*. Insertional mutations in either *ptLPD1* or *ptLPD2* genes, the only two genes that encode the LPD located in *Arabidopsis* plastids (Heazlewood et al. 2007), caused increased sensitivity to both As(V) and As(III) medium compared to wild-type (WT) plants (Chen et al. 2010). Plastidial LPD is the E3 subunit of the plastidial PYRUVATE DECARBOXYLASE COMPLEX (ptPDC) that is largely responsible for producing acetyl-coenzyme A for fatty acid biosynthesis in the plastid (Dörmann 2007). The finding that ptLPD activity in isolated plastids is sensitive to As(III), but not As(V) suggests that the increased As sensitivity in the mutants could be through the direct inhibition of residual ptLPD activity by As(III). Thus, fatty acid biosynthesis was highlighted as an important target for As toxicity in *Arabidopsis*.

The two remaining genes that encode LPD in *Arabidopsis*, the nuclear *mitochondrial LPD1* (*mtLPD1)* and *mtLPD2* genes (Lutziger & Oliver 2001), encode proteins that are found only in the mitochondria (Heazlewood et al. 2007). These LPD isoforms are 93% identical to each other at the amino acid level, but are only about 36% identical in sequence to ptLPD1 and ptLPD2. The mtLPDs are part of four multienzyme complexes that play crucial roles in oxidative carbon metabolism. The PYRUVATE DEHYDROGENASE COMPLEX (PDC) links cytosolic glycolysis with the mitochondrial citric acid cycle through oxidative decarboxylation of pyruvate to acetyl-CoA. The 2-OXOGLUTARATE DEHYDROGENASE COMPLEX (OGDC) catalyses the oxidative decarboxylation of 2-oxoglutarate (2-OG) to succinyl-CoA, a rate-limiting step in the citric acid cycle (Araújo et al. 2008). The BRANCHED-CHAIN 2-OXOACID DECARBOXYLASE COMPLEX (BCOADC) catalyses the oxidative decarboxylation of branched-chain 2-oxoacids derived through the deamination of leucine, isoleucine and valine (Taylor et al. 2004; Binder, Knill & Schuster 2007). The catabolism of branched-chain 2-oxoacids may provide an alternative energy source during severe plant stress (Fujiki et al. 2001). The mtLPD-containing GLYCINE DECARBOXYLASE COMPLEX (GDC), together with SERINE HYDROXYMETHYLTRANSFERASE, catalyses the oxidative decarboxylation of Gly to Ser. GDC is not only a key component for the photorespiratory recycling of 2-phosphoglycolate, but also plays an indispensable role in other metabolic processes (Mouillon et al. 1999; Engel et al. 2007). The NADH produced by these four complexes is the main source of reductive potential energy that is harvested by oxidative phosphorylation to produce ATP. The loss of any of these activities would adversely affect cellular energy status and could have dramatic downstream consequences for cellular metabolism. The two mtLPD proteins have been proposed to be interchangeable among these four complexes, and previous analysis indicated that disruption of *mtLPD2* has no apparent effect on *Arabidopsis* function (Lutziger & Oliver 2001).

We hypothesised that *mtlpd2* insertional mutants of *Arabidopsis*, like their *ptlpd1* and *ptlpd2* counterparts, would have increased sensitivity to both As(V) and As(III). If this were the case it would implicate distinct enzymes with the same function in plastids and mitochondria in the modulation of As sensitivity in plants. Given the central role of mtLPD2 in oxidative metabolism leading to ATP production in both photosynthetic and non-photosynthetic tissues, we further hypothesised that exposure of *mtlpd2* mutants to As(V) would more profoundly disrupt cellular oxidative metabolism than might be the case in wild-type plants. An understanding of the effects of As(V) on plant cellular metabolism through the analysis of *mtlpd2* mutants may provide insights into the molecular basis for As toxicity in plants.

MATERIALS AND METHODS

Plant materials and growth conditions

The *Arabidopsis thaliana mtlpd2-1* mutant (Lutziger & Oliver 2001) and the corresponding Wassilewskija (Ws) wild-type were kindly provided by Professor David Oliver (Iowa State University, USA). The *mtlpd2-2* mutant (SALK_027039; Alonso et al. 2003) in the Columbia (Col-0) background was obtained from the *Arabidopsis* Biological Resource Center. PCR with gene-specific primers (lpd2F1 and lpd2R1, Supporting Information Table S1) and T-DNA left border primers (LB102A for *mtlpd2-1*; LBa1 for *mtlpd2-2*, Supporting Information Table S1) was used to confirm the T-DNA insertion alleles of *mtlpd2-1* and *mtlpd2-2*. All seed were produced at the same time, and collected and stored in the same way. Seed sterilisation and growth conditions were described previously (Chen et al. 2010). For liquid culture, surface-sterilised seeds were stratified at 4°C for 2 d before carefully floating them in jars on the surface of sterile Gamborg's B-5 medium (Phytotechnology Laboratories) supplemented with 2% (w/v) sucrose and 0.08% (w/v) bacteriological grade agar (Amresco), pH 5.8. Seedlings were grown at 22°C with a 16-h-light (70 μmol photons m^{-2} s^{-1}) / 8-h-dark cycle and constant shaking at 60 rpm.

Vector construction and *Arabidopsis* transformation

Gateway™ technology (Invitrogen) was used to generate vectors for plant transformation. PCR was used to amplify a 2.2-kb promoter-containing fragment of *mtLPD2* (primers chen45F and chen45R, Supporting Information Table S1) from *Arabidopsis* genomic DNA. The PCR product was transferred into pDONR221 (Invitrogen) and the sequences confirmed before moving into the plant expression vector pMDC163 (Curtis & Grossniklaus 2003) to generate pMDC163:mtLPD2Pro, an *mtLPD2* promoter-GUS fusion. The final plasmid was introduced by electroporation into *Agrobacterium tumefaciens* strain GV3101 and transferred into Col-0 plants by the floral dip method (Clough & Bent 1998). Seeds transformed with the plasmid were selected on solid MS medium (Phytotechnology Laboratories) containing 20 μg mL^{-1} hygromycin.

Immunodetection of LPD

Mitochondria were isolated from 2-wk-old seedlings grown in liquid culture (Sweetlove, Taylor & Leaver 2007). Protein concentrations were determined using a commercial kit (Pierce Coomassie Plus Protein Assay Reagent, Thermo Fisher Scientific, Scoresby, Victoria, Australia) according to the manufacturer's instructions using BSA as the standard. Approximately 50 μg of mitochondrial protein was separated on 10 to 20% (w/v) pre-cast Tris-HCl polyacrylamide gradient gels (Bio-Rad Laboratories) and electroblotted onto a nitrocellulose membrane (Towbin, Staehelin & Gordon 1979). Membranes were incubated with polyclonal antibodies raised against the *Pisum sativum* mtLPD (Conner, Krell & Lindsay 1996) or lipoic acid (Humphries & Szweda 1998). Chemiluminescence detection and quantification was as described (Taylor et al. 2004).

Analytical methods

Arsenic was determined by inductively coupled plasma optical emission spectrometry and anthocyanin was determined spectrophotometrically in plant tissues as described (Chen et al. 2010). LPD activity was measured in the forward direction as the dihydrolipoamide-dependent reduction of NAD^+ and in the reverse direction as the

lipoamide-dependent oxidation of NADH. The reaction medium contained 50 mM TES-KOH (pH 7.5), 2 mM $MgCl_2$, 0.5% (v/v) Triton X-100, and 4 μg mL^{-1} mitochondria. For the forward reaction, the medium was supplemented with 1 mM NAD^+ and 0.1 mM D,L-dihydrolipoamide (Calbiochem), while for the reverse reaction, the medium contained 0.2 mM NADH and 1 mM D,L-α-lipoamide (Sigma-Aldrich). All reactions were initiated by adding mitochondria and monitored at 340 nm (U-2810 Dual-Beam Spectrophotometer, Hitachi, North Ryde, NSW, Australia). The change in absorbance at 340 nm was used to determine LPD activity. The effects of As(V) and As(III) on LPD activity were determined using the reverse reaction to prevent the reaction of As(III) with D,L-dihydrolipoamide.

Histochemical GUS assay

GUS histochemical staining was performed according to the method of Jefferson, Kavanagh & Bevan (1987). Seedlings grown vertically on plates containing solid medium were transferred to 1.5 mL tubes containing a solution of 100 mM sodium phosphate, pH 7.0, 10 mM EDTA, 0.5 mM potassium ferricyanide, 0.5 mM potassium ferrocyanide, 0.1% Triton X-100 and 1 mM 5-bromo-4-chloro-3-indolyl glucuronide. The seedlings were infiltrated twice by briefly applying and releasing a vacuum before incubating for 10 hours at 37°C in the dark. Chlorophyll was extracted from stained tissues by washing with several changes of 70% (v/v) ethanol.

Metabolite extraction and GC-MS analysis

Approximately 40 mg plant tissue were ground to a fine powder under liquid nitrogen and extracted with 500 μL 87% (v/v) methanol containing 8.7 μg mL^{-1} ribitol for 20 min at 75°C with 1,200 rpm shaking. Cell debris was collected by centrifugation for 3 min at 20°C with 12,000 x g. A 100 μL portion of the supernatant was dried under vacuum. The dried material was re-dissolved in 20 μL freshly-made 20 mg mL^{-1} methoxyamine hydrochloride in anhydrous pyridine and derivatised for 90 min at 37°C with 750 rpm shaking. A second derivatisation was done by adding 30 μL N-methyl-N-(trimethylsilyl)trifluoroacetamide and

190 incubating for 30 min at 37°C with 750 rpm shaking. Each sample and blank was spiked with
191 10 µL *n*-alkane retention index calibration mixture (0.07% [v/v] each *n*-dodecane,
192 *n*-pentadecane, *n*-nonadecane, *n*-docosane, *n*-octacosane, *n*-dotracontane and
193 *n*-hexatriacontane in anhydrous pyridine) and incubated at 37°C for 5 min with 750 rpm
194 shaking.
195
196 For metabolite analysis, 1 µL of the derivatised sample was injected splitless into a gas
197 chromatograph (7890A gas chromatograph fitted with an 5975C inert XL MSD with
198 Triple-Axis Detector, Agilent and a MPS2 XL-Twister autosampler, Gerstel) fitted with a
199 capillary column (0.25 mm i.d., 0.25 µm film thickness, 30 m with 10 m integrated guard,
200 Varian, FactorFour VF-5MS). Helium was used as the carrier gas at a constant flow of 1.1657
201 mL min^{-1}. The inlet temperature was set at 300 °C. The oven temperature was initially set at
202 70°C for 1 min, ramped at 1°C min^{-1} to 76°C, 6°C min^{-1} to 325°C and held for 8 min, before
203 being ramped down at 120°C min^{-1} to 70°C and held for 1.375 min. The transfer line
204 temperature was 250°C, the MS quadrupole temperature was 150°C and the source
205 temperature was 230°C. The mass detection range was set from 50 to 650 atomic mass units.
206 This analysis did not detect pyruvate, lactate or succinyl-CoA and was unable to distinguish
207 between glutamate and glutamine, or between citrate and isocitrate.
208
209 **GC-MS data analysis**
210 Six replicates of each sample were subjected to GC – MS. To analyse the data, retention
211 times were transformed into retention time indices by using the alkanes spiked into each
212 sample and the blank followed by deconvolution (Automated Mass Spectral Deconvolution
213 and Identification System software, ver. 2.64, National Institute of Standards and Technology)
214 and peak identification using an in-house library derived by analysis of known compounds.
215 The outputs were aligned (ID-Align, Computations Systems Biology, www.ce4csb.org) using
216 the integrated area of each peak for the calculations. Before comparing results, peaks areas
217 were normalised to the internal standard and sample mass. For some metabolites, a peak area

of zero was returned for one or more replicates. When zero was returned for three or fewer replicates, the mean of the non-zero replicates was reported (Supporting Information Table S2). Otherwise, a value of zero was recorded. A Student's t-test was used to determine if two means differed ($p < 0.05$ or $p < 0.01$) (Supporting Information Table S2). To compare metabolite amounts between treatments when one of the means was zero, the zero was converted to 0.01, the lowest non-zero peak area recorded.

RESULTS

Arabidopsis mtlpd2 mutants have enhanced As(V) sensitivity

We previously mapped a mutation that confers an *As(V) overly-sensitive* (*aos*) phenotype in *Arabidopsis* to the *ptLPD1* (At3g16950) gene (Chen et al. 2010). During this fine mapping on chromosome 3, the T-DNA insertion line SALK_027039 was found to also have an *aos* phenotype. To further characterise this mutant, the T-DNA insertion site in SALK_027039 was determined precisely by PCR and DNA sequencing of the PCR product to be located in the second exon of At3g17240 (Supporting Information Fig. S1a, b). This is the locus for the *mtLPD2* gene, which encodes a protein with a function related to that of ptLPD1 but that is located in mitochondria rather than plastids. The *mtLPD2* mutant allele in SALK_027039 was designated *mtlpd2-2* to differentiate it from another *mtlpd2* allele (designated *mtlpd2-1* here) previously isolated by Lutziger & Oliver (2001).

The *aos* phenotype was originally defined by the increased inhibition of root elongation in mutants exposed to As(V) compared to WT seedlings (Chen et al. 2010). Root elongation in *mtlpd2-2* seedlings in the absence of As(V) was the same as in Columbia (Col-0) WT seedlings (Fig. 1a), while exposure to various concentrations of As(V) inhibited root growth more in the mutant than in WT seedlings (Fig. 1a, b). The genetic basis of the *aos* phenotype in *mtlpd2-2* was determined by backcrossing homozygous *mtlpd2-2* to Col-0 WT. Root growth in the 50 F_1 seedlings tested was no more sensitive to As(V) than that in WT seedlings, demonstrating that *mtlpd2-2* was recessive. The *aos* phenotype in the F_2 progeny

246 from self-fertilised heterozygous F_1 plants segregated in a 1 : 3 ratio (40 *aos* : 112 WT)
247 according to the chi-square test ($p > 0.05$), indicating that the *aos* phenotype was inherited as
248 a single Mendelian locus. All 40 seedlings that showed the *aos* phenotype in the F_2
249 generation were homozygous by PCR for the T-DNA insertion that created the *mtlpd2-2*
250 allele, demonstrating that the T-DNA insert co-segregated with the *aos* phenotype.
251
252 To confirm that disruption of *mtLPD2* was responsible for the *aos* phenotype, we tested root
253 elongation in *mtlpd2-1* seedlings for sensitivity to As(V). The *mtlpd2-1* allele has two
254 T-DNA insertions that did not segregate over several generations (Lutziger & Oliver 2001)
255 and are inserted in *mtLPD2* as inverted repeats (LB–T-DNA–T-DNA–LB; Supporting
256 Information Fig. S1a, b). On As(V)-free medium, root elongation in the mutant was the same
257 as in the corresponding Ws WT (Fig. 1a). At all As(V) concentrations tested, primary root
258 growth in *mtlpd2-1*seedlings, like that in *mtpld2-2* seedlings, was more strongly inhibited
259 than in WT (Fig. 1b). This observation supports the conclusion that disruption of *mtLPD2*
260 confers increased sensitivity of root elongation to As(V). RT-PCR analyses showed that there
261 were no detectable *mtLPD2* transcripts in either *mtlpd2-1* or *mtlpd2-2* (Supporting
262 Information Fig. S1c), indicating that both mutants contained knockout alleles. The
263 sensitivity of *mtlpd2-2* to As(V) was restored to WT levels by introducing a Col-0 WT
264 genomic fragment encompassing *mtLPD2* (Supporting Information Fig. S2) confirming that
265 the *aos* phenotype in *mtlpd2-2* was due to disruption of *mtLPD2*.
266
267 The As(V) sensitivity of lines carrying *mtlpd2* alleles was quantified by estimating the
268 concentration of As(V) that decreased root elongation by 50% (I_{50}) (Chen et al. 2010).
269 *Arabidopsis* Ws had an I_{50} for As(V) toward root growth of approx. 260 μM. Thus, Ws was
270 more sensitive to As(V) than Col-0, which had an I_{50} of greater than 400 μM. This result
271 indicates that there is at least one other naturally polymorphic locus in *Arabidopsis*
272 contributing to the As(V) sensitivity of the two accessions. Disrupting *mtLPD2* in Ws
273 (*mtlpd2-1*) and Col-0 (*mtlpd2-2*) backgrounds decreased the estimated I_{50} to about 150 μM

and 250 μM, respectively, an equivalent proportional decrease of about 1.7-fold compared with the I_{50} of the corresponding WT.

In the absence of As(V), Col-0 had a greater number of lateral roots than Ws (Fig. 1c). Exposure to 100 μM As(V) caused the formation of fewer lateral roots in both Col-0 and Ws, with the reduction being more severe for Col-0. Conversely, As(V) concentrations above 100 μM stimulated the growth of lateral roots in Ws and did not inhibit lateral root proliferation in Col-0 as severely as 100 μM As(V). Both *mtlpd2-1* and *mtlpd2-2* had fewer lateral roots than the corresponding WT in the absence of As(V). However, when exposed to 100 μM As(V), *mtlpd2-1* and *mtlpd2-2* produced 1.8 and 2.3 times more lateral roots, respectively, than the corresponding WT. Exposure to 200 μM As(V) also caused both mutants to produce more lateral roots than WT, but the difference was less than at 100 μM As(V). Interestingly, both mutants had similar numbers of lateral roots, regardless of the genetic background, unlike the two WT lines.

The effect of As(V) on shoot growth in *mtlpd2* was determined by exposing uniformly sized 5-d-old seedlings to As(V)-containing growth media for two weeks. In the absence of As(V), the mutants were smaller and had slightly lower fresh weights than the corresponding WT (Fig. 2a; Supporting Information Fig. S3). Exposure to various concentrations of As(V) caused a decrease in fresh weight in WT, a decrease that was stronger in the mutants (Fig. 2a). At each As(V) concentration tested, the mutants produced less than half the fresh weight of the corresponding WT. Moreover, the mutants accumulated more anthocyanin in the aerial tissues than did WT (Fig. 2b), an indication that the mutants were more sensitive the stress induced by As(V) exposure than the corresponding WT.

mtLPD2 has a tissue-dependent expression pattern

Lutziger & Oliver (2001) showed by northern blot analysis that *mtLPD2* transcripts accumulate in roots, stems, leaves, flowers, and siliques of mature *Arabidopsis*. The

tissue-dependent expression pattern of *mtLPD2* was investigated in more detail by fusing the 2.2-kb genomic DNA fragment from immediately upstream of the *mtLPD2* initiation codon directly upstream of the *GUS* reporter gene, and introducing the construct into *Arabidopsis*. GUS activity was detected in cotyledons, rosette leaves, and roots (Fig. 3). Activity was not strongly expressed in the hypocotyls (Fig. 3a) or the meristematic zone of the main or lateral roots (Fig. 3b, d) in either 5- or 12-d-old seedlings. Interestingly, GUS expression was clearly visible in the cap of the established lateral roots (Fig. 3e), but not in the cap of the main root (Fig. 3d) or newly initiated lateral root (Fig. 3f).

The *mtlpd2-2* mutant does not over-accumulate As

The As concentration in the tissues of plants exposed to As(V) was determined to clarify whether the *mtlpd2*-dependent *aos* phenotype was simply due to over-accumulation of As. Only *mtlpd2-2* was used in these experiments as both *mtlpd2* alleles conferred equal sensitivity to As(V) compared to the respective WT. The *mtlpd2-2* mutant and Col-0 WT had similar shoot As concentrations on a dry weight basis (Fig. 4a). Surprisingly, the roots of the mutant accumulated less As than those of WT (Fig. 4b). Together, these results indicate that the *aos* phenotype of *mtlpd2* was not due to increased accumulation of As in the tissues.

***mtlpd2* has decreased mtLPD protein and activity**

Since two nuclear genes encode mtLPD in *Arabidopsis* (Lutziger & Oliver 2001, Heazlewood et al. 2007), it was of interest to know the impact of the observed loss of *mtLPD2* transcripts on mtLPD abundance and activity. The mtLPD protein was detected on immunoblots of mitochondrial proteins isolated from WT and *mtlpd2-2* seedlings grown in liquid culture. The immunoblots were probed with an anti-*Pisum sativum* LPD antiserum, which was expected to interact with *Arabidopsis* mtLPD, since the proteins from the two species share 85% identity at the amino-acid sequence level (Lutziger & Oliver 2001). A single immunoreactive band was detected at 55 kDa in mitochondria from WT *Arabidopsis* (Fig. 5a). This band is likely to contain both mtLPD1 and mtLPD2, since each protein has

507 amino acids and a calculated molecular mass of 54 kDa. Analysis of mitochondria from *mtlpd2-2* also produced a single immunoreactive band at 55 kDa, but the intensity of the signal was about 25% lower than the intensity of the corresponding band from the same amount of mitochondria from the WT (Fig. 5a). Mitochondria isolated from the *mtlpd2-2* mutant also had decreased mtLPD-specific activity in reactions run in either the forward or reverse direction (Fig. 5a, b). Together, these results indicate that the loss of *mtLPD2* gene activity caused a decrease in total mtLPD activity, but did not abolish it.

The mtLPD protein is a subunit of four mitochondrial enzyme complexes. Each complex possesses three subunits, E1, E2 and E3 (mtLPD), that are functionally analogous across the complexes. In each complex, mtLPD accepts electrons from a dihydrolipoic acid moiety attached to the E2 subunit of the same complex. This arrangement raises the possibility that the *aos* phenotype could be a consequence of an *mtlpd2*-dependent decrease in the abundance of the E2 subunits or their lipoic acid prosthetic group. The possible pleiotropic decrease in E2 abundance in the mutant was examined by immunoblotting mitochondria from *mtlpd2-2* and WT seedlings with polyclonal antibodies that specifically recognize the lipoic acid moiety of E2, which provides the substrate of mtLPD. A similar amount of lipoic acid was found to be associated with the E2 subunits of the PDC and OGDC in mitochondria isolated from both the mutant and WT (Supporting Information Fig. S4). The E2 subunit of BCOADC was typically not detected in these immunoblots due to its low abundance (Taylor et al. 2004), while the 12 kDa H subunit of GDC was smaller than the MW range resolved on the gel.

As(III), not As(V), inhibits mtLPD and is the likely mediator of the *aos* phenotype in *mtlpd2*

The high affinity of As(III) toward dithiol groups was originally used to demonstrate the involvement of two vicinal disulfide groups in the LPD catalytic cycle (Massey & Veeger 1960). These and subsequent studies revealed that LPD from bacteria, porcine heart, and *Arabidopsis* plastids was inactivated by As(III) (Massey & Veeger 1960; Marcinkeviciene &

358 Blanchard 1997; Chen et al. 2010). The effects of As(III) and As(V) on *Arabidopsis* mtLPD
359 activity was measured in isolated mitochondria using NADH and lipoic acid as substrates.
360 The assays were run in the direction of NADH oxidation and dihydrolipoamide formation.
361 The mtLPD was sensitive to As(III) with an I_{50} (concentration required for 50% inhibition of
362 activity) for As(III) estimated to be about 25 μM (Fig. 6a). The mtLPD activity was not
363 influenced by 1 mM As(V) when assayed in the direction of NADH oxidation (Fig. 6b).
364
365 If the enhanced As(V) sensitivity of *mtlpd2* is mediated by As(III) inactivation of LPD,
366 *mtlpd2* would be expected to be overly-sensitive to As(III). Root elongation in *mtlpd2-2*
367 seedlings was indeed more sensitive to As(III) than in WT (Fig. 7a). Exposure of young
368 seedlings to 5 μM As(III) inhibited root elongation by 60% in *mtlpd2-2*, but only by 10% in
369 WT. The I_{50} of As(III) with respect to root elongation in *mtlpd2-2* was about 4 μM. Fresh
370 weight accumulation in *mtlpd2-2* was also more sensitive to As(III) than in WT (Fig. 7b).
371
372 **Mutation of *mtLPD2* enhanced As(V)-induced changes in metabolite pools**
373 Metabolite profiling was performed on shoot and root tissues of 15-d-old WT and *mtlpd2-2*
374 plants grown in the presence or absence of As(V) for 9 d before harvest. This As(V)
375 treatment was relatively mild, as plants did not show visible signs of toxicity. Sixty-eight
376 metabolites were reproducibly identified in samples from both genotypes by gas
377 chromatography-mass spectrometry (GC-MS) and compared by Student's *t*-test ($p < 0.05$)
378 (Supporting Information Table S2). Some metabolites were not detected in all replicates of
379 each tissue sample.
380
381 The abundance of most of the detected compounds did not differ appreciably between WT
382 and the *mtlpd2-2* mutant. An exception was that the abundance of 2-OG, the substrate for
383 LPD-containing OGDC, was 35% higher ($p < 0.05$) in roots and 40% higher ($p < 0.01$) in
384 shoots of the *mtlpd2-2* mutant than in the corresponding WT tissue (Supporting Information
385 Table S2). The abundance of the substrates for LPD-containing GDC and BCOADC, Gly, Ile,

386 Leu and Val, were not appreciably different in the mutant. Pyruvate, the substrate for PDC,
387 could not be detected by our analysis method. The amounts of the detected citric acid cycle
388 intermediates citrate / isocitrate, succinate, fumarate and malate were also unaltered in both
389 *mtlpd2-2* roots (Fig. 8) and shoots (Supporting Information Table S2).
390
391 Exposure of WT plants to 200 μM As(V) dramatically affected the abundance of several
392 metabolites, particularly amino acids (Fig. 8, Supporting Information Table S2). In roots of
393 As(V)-treated WT plants, the abundance of Ala increased to the greatest extent of any of the
394 detected metabolites. Several other amino acids were also more abundant in these roots,
395 especially Gly, Ser, Thr, γ-aminobutyric acid (GABA) and Glu / Gln. Lys, which was below
396 the limit of detection in roots from untreated WT, was easily detected upon As(V) treatment.
397 The roots from treated plants also had at least 2-fold more 2-OG than those from untreated
398 plants (Fig. 8). This increase in 2-OG was not accompanied by changes in the abundance of
399 any other citric acid cycle intermediates. Roots from As(V)-treated WT plants had higher
400 amounts of the oxidative stress indicator ascorbate. In WT shoots, the As(V)-induced
401 differences in steady-state metabolite pools were similar to, but much less pronounced than
402 those in roots (Supporting Information Table S2). Notably, compared to the roots, the shoots
403 of As(V)-treated plants had a greater increase in the abundance of benzoate and substantially
404 less pronounced increases in Ala, Ser, Thr, GABA, Lys and 2-OG.
405
406 The metabolite pools in both the roots and shoots of *mtlpd2-2* plants generally responded
407 similarly, but more strongly, to 200 μM As(V) than those in the WT tissues (Fig. 8,
408 Supporting Information Table S2). As in the WT, the majority of compounds that
409 accumulated in roots of As(V)-treated *mtlpd2-2* were amino acids, but the increases were
410 generally greater in the mutant than in the WT. The smaller increase in the amount of Ala
411 was a notable exception. Interestingly, of the amino acids detected, Asp was the only one that
412 did not change in abundance, while Tyr was the only one to decrease in abundance, upon
413 As(V) treatment in both the WT and the mutant. In roots of As(V)-treated *mtlpd2-2*, 2-OG

levels were 19-fold higher than in the untreated mutant, which was an 8-fold greater increase in abundance than seen in roots of As(V)-treated WT (Supporting Information Table S2). As was the case in the WT, other citric acid cycle intermediates did not accumulate to higher levels in the mutant upon As(V) treatment.

The As(V)-induced alteration of metabolite pools in *mtlpd2-2* shoots was quite distinct from that in the roots. Instead of an extensive remodelling of amino acid pools, there was an enhancement of metabolites associated with carbon metabolism, such as fructose, glucose, glycerate, glycolate and gluconate. The only amino acids that accumulated to any degree in shoots of As(V)-treated *mtlpd2-2* were Asn, Gly, Pro and GABA. Interestingly, Asp levels in both roots and shoots of *mtlpd2-2* were unchanged by As(V) treatment, while Asp was more abundant in both tissues from As(V)-treated WT.

DISCUSSION

mtLPD is typically in excess to metabolic requirements.

The lack of a strong growth phenotype in *mtlpd2-2 Arabidopsis* under typical growth conditions confirmed the earlier conclusion that *mtLPD1* expression can satisfy the physiological requirements of the plant (Lutziger & Oliver 2001). Although both genes are expressed in most tissues, *mtLPD1* transcripts and protein predominated in leaves, while transcripts and protein from both genes were more similar in abundance in roots (Lutziger & Oliver 2001, Baerenfaller et al. 2008, Lee et al. 2011). The exception was in the root tip, where microarray data (GENEVESTIGATOR, Zimmermann et al. 2004) shows that *mtLPD1* transcripts are two-fold more abundant that those from *mtLPD2*. This nuance is supported by our finding that the *mtLPD2* promoter was active throughout the root, except in the meristematic zone of all roots and the root cap of the main and newly initiated lateral roots. Consequently, the contribution of *mtLPD2* to mitochondrial function was generally in excess to the physiological needs of the plant in the absence of As(V).

443 It is intriguing that As(V) caused a much stronger shift in resource allocation from primary
444 root elongation to lateral root formation in the *mtlpd2* mutants than in the WT lines. Perhaps
445 the root apical meristem of the main root in the mutants was more sensitive to As(V) than the
446 cells in the lateral root primordia. Microarray data indicated that there is cell-type dependent
447 variation in both the proportion and absolute amounts of *mtLPD1* and *mtLPD2* transcripts in
448 *Arabidopsis* roots (GENEVESTIGATOR, Zimmermann et al. 2004, Brady et al. 2007).
449 Perhaps these differences in *mtLPD1* gene expression patterns are enough in the absence of
450 *mtLPD2* to change the metabolic balance within the root and cause the altered response of
451 root growth to As(V).
452
453 The lack of extensive metabolome remodelling in the *mtlpd2-2* mutant in the absence of
454 As(V) was consistent with the physiological redundancy of *mtLPD2*. However, the increase
455 in the steady-state level of 2-OG in *mtlpd2-2* under typical growth conditions compared to
456 WT suggests restriction of OGDC activity in the mutant, consistent with decreased mtLPD2
457 activity. The small increase in the 2-OG concentration, but not in the concentration of
458 metabolites linked to PDC, GDC or BCOADC activities, support the view that OGDC is a
459 major control point for respiration in plants (Plaxton & Podestá 2006; Araújo et al. 2008).
460 LPD is also known to have a lower binding affinity for OGDC than PDC in plants, with
461 OGDC losing nearly all its associated LPD during purification. OGDC activity in thus likely
462 to be more dependent on mtLPD concentration than PDC in plants (Millar, Hill & Leaver
463 1999).
464
465 Previous work showed that *mtlpd2-1* roots respired exogenous pyruvate to the same extent as
466 WT roots (Lutziger & Oliver 2001). Pyruvate was not detectable in our GC-MS approach.
467 However, Ala accumulation is likely a good general indicator of decreased pyruvate
468 metabolism in plant roots. Pyruvate is linked to Ala through alanine aminotransferase and
469 GABA transaminase, and the respective amino group donors Glu and GABA. Ala
470 accumulates when mitochondrial respiration is compromised by chemical inhibition (Araújo

et al. 2008; Garmier et al. 2008), by genetic knockout (Meyer et al. 2009) or by low oxygen availability (Narsai et al. 2009; van Dongen et al. 2009; Rocha et al. 2010; Shingaki-Wells et al. 2011). Thus, the lack Ala accumulation in the *mtlpd2-2* mutant under typical growth conditions suggests that pyruvate metabolism was not severely compromised, as was also true in the *mtlpd2-1* mutant (Lutziger & Oliver 2001).

The *aos* phenotype is not due to increased As accumulation

The As concentration in the roots and shoots of *mtlpd2* plants exposed to As(V) was never higher than that in WT control plants, as was also the case for the *ptlpd1* mutant that we previously characterised (Chen et al. 2010). Therefore, the increased As(V) sensitivity of both mutants was not due to a tissue-wide increase in As burden. Thus, it seems likely that the *aos* phenotype of both *mtlpd2* and *ptlpd1* mutants was directly due to the lower LPD activity. However, we do not know whether the partitioning of As(V) within the tissues was changed within the mutants compared to WT. As(V) sensitivity can be associated with low As accumulation, while As-tolerant phenotypes can be associated with enhanced As content (Meharg & Macnair 1990, Catarecha et al. 2007). This apparent paradox is likely due to the fact that resistant plants often have slower As(V) up-take rates, allowing more time for As detoxification in the cytosol and sequestration in the vacuole. Thus, it is possible that decreased LPD activity leads to a change in the detoxification efficiency, exposing As-sensitive processes to higher doses of As. Mass spectrometry experiments compiled at the SUBA website (Heazlewood et al. 2007) strongly suggest that mtLPD and ptLPD enzymes are targeted specifically to mitochondria and plastids, respectively. In the case of ptLPD2, this conclusion is supported by *in vivo* targeting experiments (Drea et al. 2001). Thus, LPD in both mitochondrial and plastid compartments contribute to determining As(V) sensitivity in *Arabidopsis*.

The mechanism by which As(V) in the growth medium exerted its enhanced toxicity on the *mtlpd2-2* mutant was not clear. The accumulation of the substrates for OGDC, BCOADC and

499 GDC in *mtlpd2* compared to that in WT in response to As(V) exposure suggested that the *aos*
500 phenotype was linked to inhibition of these enzymes. However, mtLPD activity was
501 insensitive to As(V), ruling out direct inhibition of these enzyme complexes. In plants, As(V)
502 can be readily reduced to As(III), which is a potent inhibitor of mtLPD, offering one possible
503 mechanism leading to the *aos* phenotype. On the other hand, plants exposed to As produce
504 ROS (Finnegan & Chen 2012), which is able to initiate the breakdown of subunits of PDC,
505 OGDC, several other enzymes of the citric acid cycle and GABA aminotransferase
506 (Sweetlove et al. 2002). In animals, the amount of As(III) that is required to inactivate
507 LPD-containing PDC *in vivo* through the production of ROS is much lower than that needed
508 to directly inhibit the enzyme *in vitro* (Samikkannu et al. 2003). While similar experiments
509 have not been carried out in a plant system, these results from a human cell-culture system
510 indicate that the ROS-dependent pathway may have mediated the disruption of metabolism
511 by As(V) at the sites of LPD and that this disruption requires the reduction of As(V) to
512 As(III). Regardless of which of these mechanisms was involved, the observations that both
513 As(III) and As(V), albeit at different concentrations, elicited the same *aos* phenotype in
514 *mtlpd2-2* was consistent with both forms of As acting through a single mechanism that was
515 enhanced by lower mtLPD expression.
516
517 **As(V) exposure alters oxidative metabolism in *Arabidopsis***
518 Extended As(V) exposure radically altered oxidative metabolism in both roots and shoots of
519 WT *Arabidopsis*. In roots, the changes were largely focused on amino acids associated with
520 the TCA cycle, while in shoots the changes were associated more with components of the
521 oxidative stress response. Surprisingly, these large-scale adjustments to metabolism did not
522 result in obvious toxicity symptoms. The As(V) effects were stronger in roots than in shoots.
523 This was most likely due to the pronounced accumulation of As in roots over shoots that was
524 observed here and elsewhere (Quaghebeur & Rengel 2004; Raab et al. 2007). The retention
525 of As in the roots can be explained at least in part by the *in planta* metabolism of As (Zhao et
526 al. 2009; Finnegan & Chen 2012).

Mild As(V) treatment caused large changes in amino and organic acid pools that were exacerbated by the decrease in mtLPD activity in *mtlpd2* roots This observation highlights longstanding questions regarding the source of these amino acids and why some of those metabolically linked to 2-OG, such as Ala, Glu / Gln, Pro and GABA, have repeatedly been found to accumulate in response to various challenges. The dramatic accumulation of Ala upon As(V) exposure suggests that pyruvate metabolism is a prime target for As(V) toxicity in plants, as in animals (Hughes 2002; Hughes et al. 2011). The transamination of pyruvate to Ala, using either Glu or GABA as the amino donor, does not involve the oxidation of NADH, and so would not itself be a fermentative reaction that is able to support glycolysis. Instead, accumulated Ala may have acted as a carbon / nitrogen reserve to be used during recovery from the stress or to regulate the amount of pyruvate that was fermented to lactate or ethanol (Good & Crosby 1989; Miyashita et al. 2007). OGDC and the associated metabolic reactions also appeared to be an important target for chronic As(V) toxicity. The strong increases in 2-OG, Ala, Glu/Gln, and Gly levels in As(V)-treated roots resembled the changes seen in potato tubers, another heterotrophic tissue, treated with OGDC-specific inhibitors (Araújo et al. 2008). The high levels of Glu and 2-OG may also reflect changes in the C / N balance in the tissue (Plaxton & Podestá 2006).

Taken together, the metabolite abundance data indicate that the lower mtLPD activity in *mtlpd2* altered oxidative metabolism within tissues, especially the root. The new metabolic poise of the mutant tissue, then, would have been nearer to an undefined threshold of mtLPD activity. The weak visible phenotype and the modest adjustments to metabolite pools that occurred in the mutant in the absence of As(V) indicate that it was only in the presence of As that the mtLPD activity threshold was breached. The profound effect that As(V) treatment had on the abundance of oxidative metabolites downstream of pyruvate in *mtlpd2* roots, provides important areas for further study to determine the primary cause of As toxicity in plants.

In conclusion, mtLPD was found to be an *in vivo* contributor to As(V) sensitivity in *Arabidopsis*. The As(V) hypersensitivity of the *mtlpd2* knock-out mutants probably came about by enhanced sensitivity of plant central metabolism. In combination with our analysis of *ptlpd* mutants (Chen et al 2010), it is now clear that enzymes with similar functions in multiple locations in the cell are central components of an As toxicity mechanism in plants. These should represent a key focus for biotechnological efforts to safeguard the metabolism of plants being developed for environmental As remediation.

Acknowledgements

We thank Professor David Oliver (Iowa State University, USA) for providing the *Arabidopsis mtlpd2-1* mutant, Michael Smirk (School of Earth and Environment, The University of Western Australia) for his assistance in quantifying arsenic and Ricarda Fenske (Metabolomics Australia, The University of Western Australia) for her assistance with the metabolite analysis. This work was supported by an International Postgraduate Research Scholarship from the Australian Government, Department of Education, Employment and Workplace Relations (W.C.), a University Postgraduate Award from The University of Western Australia (W.C.), grants (P.M.F., H.L., A.H.M.) and an Australian Postdoctoral Fellowship (N.L.T.) from the Australian Research Council, and an award from the China Scholarship Council (Y.C.).

577

578 **REFERENCES**

579 Ahmed M.F., Ahuja S., Alauddin M., Hug SJ., Lloyd JR., Pfaff A., Pichler T., Saltikov C.,
580 Stute M. & van Geen A. (2006) Ensuring safe drinking water in Bangladesh. *Science*
581 **314**, 1687-1688.

582 Araújo WL., Nunes-Nesi A., Trenkamp S., Bunik VI. & Fernie A.R. (2008) Inhibition of
583 2-oxoglutarate dehydrogenase in potato tuber suggests the enzyme is limiting for
584 respiration and confirms its importance in nitrogen assimilation. *Plant Physiology* **148**,
585 1782-1796.

586 Baerenfaller K., Grossmann J., Grobei M. A., Hull R., Hirsch-Hoffmann M., Yalovsky S.,
587 Zimmermann P., Grossniklaus U., Gruissem W. & Baginsky S. (2008) Genome-scale
588 proteomics reveals *Arabidopsis* thaliana gene models and proteome dynamics.
589 *Science* **320**, 938-941.

590 Bergquist E.R., Fischer R.J., Sugden K.D. & Martin B.D. (2009) Inhibition by methylated
591 organoarsenicals of the respiratory 2-oxo-acid dehydrogenases. *Journal of*
592 *Organometallic Chemistry* **694**, 973-980.

593 Binder S., Knill T. & Schuster J**. (2**007) Branched-chain amino acid metabolism in higher
594 plants. *Physiologia Plantarum* **129,** 68-78.

595 Brady S.M., Orlando D.A., Lee J.-Y., Wang, J.Y., Koch J., Dinneny J.R., Mace D., Ohler U.
596 & Benfey, P.N. (2007) A high-resolution root spatiotemporal map reveals dominant
597 expression patterns. *Science* **318**, 801-806.

598 Catarecha P., Segura M.D., Franco-Zorrilla J.M., García-Ponce B., Lanza M., Solano R.,
599 Paz-Ares J. & Leyva A. (2007) A mutant of the *Arabidopsis* phosphate transporter
600 PHT1;1 displays enhanced arsenic accumulation. *The Plant Cell* **19**, 1123-1133.

601 Chen W., Chi Y., Taylor NL., Lambers H. & Finnegan PM. (2010) Disruption of *ptLPD1* or
602 *ptLPD2*, genes that encode isoforms of the plastidial lipoamide dehydrogenase,
603 confers arsenate hypersensitivity in *Arabidopsis*. *Plant Physiology* **153**, 1385-1397.

604 Clough S.J. & Bent A.F. (1998) Floral dip, A simplified method for Agrobacterium-mediated
605 transformation of *Arabidopsis thaliana*. *The Plant Journal* ***16****,* 735–743.
606 Conner M., Krell T. & Lindsay J.G. (1996) Identification and purification of a distinct
607 dihydrolipoamide dehydrogenase from pea chloroplasts. *Planta* **200**, 195-202.
608 Curtis M.D. & Grossniklaus U. (2003) A gateway cloning vector set for high-throughput
609 functional analysis of genes in planta. *Plant Physiology* **133**, 462-469.
610 Dhankher O.P., Rosen BP., McKinney E.C. & Meagher R.B. (2006) Hyperaccumulation of
611 arsenic in the shoots of *Arabidopsis* silenced for arsenate reductase (ACR2).
612 *Proceedings of the National Academy of Sciences of the United States of America* **103**,
613 5413-5418.
614 Dörmann P. (2007) Lipid synthesis., metabolism and transport. in The structure and function
615 of plastids., R.R. Wise and J.K. Hoober., eds. (Dordrecht, Springer)., pp. 335-353.
616 Drea S.C., Mould R.M., Hibberd J.M., Gray J.C. & Kavanagh T.A. (2001) Tissue-specific
617 and developmental-specific expression of an *Arabidopsis thaliana* gene encoding the
618 lipoamide dehydrogenase component of the plastid pyruvate dehydrogenase complex.
619 *Plant Molecular Biology* **46**, 705-715.
620 Engel N., van den Daele K., Kolukisaoglu U., Morgenthal K., Weckwerth W., Parnik T.,
621 Keerberg O. & Bauwe H. (2007) Deletion of glycine decarboxylase in *Arabidopsis* is
622 lethal under nonphotorespiratory conditions. *Plant Physiology* **144**, 1328-1335.
623 Finnegan P.M. & Chen W. (2012) Arsenic toxicity: the effects on plant metabolism. Frontiers
624 in Physiology **3**, 182.
625 Fujiki Y., Ito M., Nishida I. & Watanabe A. (2001) Leucine and its keto acid enhance the
626 coordinated expression of genes for branched-chain amino acid catabolism in
627 *Arabidopsis* under sugar starvation. *FEBS Letters* **499**, 161-165.
628 Garmier M., Carroll A.J., Delannoy E., Vallet C., Day D.A., Small I.D. & Millar A.H. (2008)
629 Complex I dysfunction redirects cellular and mitochondrial metabolism in
630 *Arabidopsis*. *Plant Physiology* **148**, 1324-1341.

631 Good A.G. & Crosby W.L. (1989) Anaerobic induction of alanine aminotransferase in barley
632 root tissue. *Plant Physiology* **90**, 1305-1309.
633 Heazlewood J.L., Verboom R.E., Tonti-Filippini J., Small I. & Millar A.H. (2007) SUBA: the
634 *Arabidopsis* Subcellular Database. *Nucleic Acids Research* **35**, D213-D218.
635 Hughes M.F. (2002) Arsenic toxicity and potential mechanisms of action. *Toxicology Letter*
636 **133**, 1-16.
637 Hughes M.F., Beck B.D., Chen Y., Lewis A.S. & Thomas D.J. (2011) Arsenic exposure and
638 toxicology, a historical perspective. *Toxicological Sciences* **123**, 305–332.
639 Humphries K.M. & Szweda L.I. (1998) Selective inactivation of alpha-ketoglutarate
640 dehydrogenase and pyruvate dehydrogenase, reaction of lipoic acid with
641 4-hydroxy-2-nonenal. *Biochemistry* **37**, 15835-15841.
642 International Agency for Research on Cancer (2004) Some Drinking-Water Disinfectants and
643 Contaminants, Including Arsenic. In *IARC Monographs on the Evaluation of*
644 *Carcinogenic Risks to Humans*. Volume 84. IARC, Vienna, Austria.
645 Jefferson R.A., Kavanagh T.A. & Bevan M.W. (1987) GUS fusions, β-glucuronidase as a
646 sensitive and versatile gene fusion marker in higher plants. *EMBO Journal* **6,**
647 3901-3907.
648 Lee C.P., Eubel H., O'Toole N. & Millar A. H. (2011) Combining proteomics of root and
649 shoot mitochondria and transcript analysis to define constitutive and variable
650 components in plant mitochondria. *Phytochemistry* **72**, 1092–1108.
651 Lutziger I. & Oliver D.J. (2001) Characterization of two cDNAs encoding mitochondrial
652 lipoamide dehydrogenase from *Arabidopsis*. *Plant Physiology* **127**, 615-623.
653 Marcinkeviciene J. & Blanchard J.S. (1997) Catalytic properties of lipoamide dehydrogenase
654 from *Mycobacterium smegmatis*. *Archives of Biochemistry and Biophysics* **340**,
655 168-176.
656 Massey V. & Veeger C. (1960) On the reaction mechanism of lipoyl dehydrogenase.
657 *Biochimica et Biophysica Acta* **40**, 184-185.

658 Meharg A.A. & Macnair M.R. (1990) An altered phosphate uptake system in
659 arsenate-tolerant *Holcus lanatus* L. *New Phytologist* **116**, 29-35.
660 Meyer E.H., Tomaz T., Carroll A.J., Estavillo G., Delannoy E., Tanz S.K., Small I.D.,
661 Pogson B.J. & Millar A.H. (2009) Remodeled respiration in *ndufs4* with low
662 phosphorylation efficiency suppresses *Arabidopsis* germination and growth and alters
663 control of metabolism at night. *Plant Physiology* **151**, 603-619.
664 Millar A.H., Hill S.A. & Leaver C.J. (1999) Plant mitochondrial 2-oxoglutarate
665 dehydrogenase complex: purification and characterization in potato. *Biochemical*
666 *Journal* **343**, 327-334.
667 Miyashita Y., Dolferus R., Ismond K.P. & Good A.G. (2007) Alanine aminotransferase
668 catalyses the breakdown of alanine after hypoxia in *Arabidopsis thaliana*. *The Plant*
669 *Journal* **49**, 1108-1121.
670 Mouillon J.-M., Aubert S., Bourguignon J., Gout E., Douce R. & Rébeillé F. (1999) Glycine
671 and serine catabolism in non-photosynthetic higher plant cells, their role in C1
672 metabolism. *The Plant Journal* **20**, 197-205.
673 Narsai R., Howell K.A., Carroll A., Ivanova A., Millar A.H. & Whelan J. (2009) Defining
674 core metabolic and transcriptomic responses to oxygen availability in rice embryos
675 and young seedlings. *Plant Physiology* **151**, 306–322.
676 Németi B., Regonesi M.E., Tortora P. & Gregus Z. (2010) Polynucleotide phosphorylase and
677 mitochondrial ATP synthase mediate reduction of arsenate to the more toxic arsenite
678 by forming arsenylated analogues of ADP and ATP. *Toxicological Sciences* **117**,
679 270–281.
680 Nordstrom D.K. (2002) Worldwide occurrences of arsenic in ground water. *Science* **296,**
681 2143-2145.
682 Plaxton W.C. & Podestà F.E. (2006) The functional organization and control of plant
683 respiration. *Critical Reviews in Plant Sciences* **25**, 159-198.
684 Quaghebeur M. & Rengel Z. (2004) Arsenic uptake., translocation and speciation in *pho1* and
685 *pho2* mutants of *Arabidopsis thaliana*. *Physiologia Plantarum* **120,** 280-286.

686 Raab A., Williams P.N., Meharg A. & Feldmann J. (2007) Uptake and translocation of
687 inorganic and methylated arsenic species by plants. *Environmental Chemistry* **4**,
688 197-203.
689 Rocha M., Licausi F., Araújo W.L., Nunes-Nesi A., Sodek L., Fernie A.R. & van Dongen J.T.
690 (2010) Glycolysis and the tricarboxylic acid cycle are linked by alanine
691 aminotransferase during hypoxia induced by waterlogging of *Lotus japonicas*. *Plant*
692 *Physiology* **152**, 1501-1513.
693 Rosen B.A., Ajees A.A. & McDermott T.R. (2011) Life and death with arsenic. *Bioessays* **33**,
694 350-357.
695 Samikkannu T., Chen C.H., Yih L.H., Wang A.S., Lin S.Y., Chen T.C. & Jan K.Y. (2003)
696 Reactive oxygen species are involved in arsenic trioxide inhibition of pyruvate
697 dehydrogenase activity. *Chemical Research in Toxicology* **16**, 409–414.
698 Shin H., Shin H.S., Dewbre G.R. & Harrison M.J. (2004) Phosphate transport in *Arabidopsis*,
699 Pht1;1 and Pht1;4 play a major role in phosphate acquisition from both low- and
700 high-phosphate environments. *The Plant Journal* **39**, 629-642.
701 Shingaki-Wells R.N., Huang S., Taylor N.L., Carroll., AJ., Zhou W. & Millar A.H. (2011)
702 Differential Molecular Responses of Rice and Wheat Coleoptiles to Anoxia Reveal
703 Novel Metabolic Adaptations in Amino Acid Metabolism for Tissue Tolerance. *Plant*
704 *Physiology* **156**, 1706–1724.
705 Sienkiewicz-Porzucek A., Sulpice R., Osorio S., Krahnert I., Leisse A., Urbanczyk-Wochniak
706 E., Hodges M., Fernie A.R. & Nunes-Nesi A. (2010) Mild reductions in
707 mitochondrial NAD-dependent isocitrate dehydrogenase activity result in altered
708 nitrate assimilation and pigmentation but do not impact growth. *Molecular Plant* **3**,
709 156-173.
710 Sweetlove L.J., Heazlewood J.L., Herald V., Holtzapffel R., Day D.A., Leaver C.J. & Millar
711 A.H. (2002) The impact of oxidative stress on *Arabidopsis* mitochondria. *The Plant*
712 *Journal* **32**, 891-904.

713 Sweetlove L.J., Taylor N.L. & Leaver C.J. (2007) Isolation of intact, functional mitochondria
714 from the model plant *Arabidopsis thaliana*. *Methods in Molecular Biology* **372**,
715 125-136.
716 Taylor N.L., Heazlewood J.L., Day D.A. & Millar A.H. (2004) Lipoic acid-dependent
717 oxidative catabolism of α-keto acids in mitochondria provides evidence for
718 branched-chain amino acid catabolism in *Arabidopsis*. *Plant Physiology* **134**,
719 838-848.
720 Towbin H., Staehelin T. & Gordon J. (1979) Electrophoretic transfer of proteins from
721 polyacrylamide gels to nitrocellulose sheets, procedure and some applications.
722 *Proceedings of the National Academy of Sciences of the United States of America* **76**,
723 4350-4354.
724 van Dongen J.T., Fröhlich A., Ramírez-Aguilar S.J., Schauer N., Fernie A.R., Erban A.,
725 Kopka J., Clark J., Langer A. & Geigenberger P. (2009) Transcript and metabolite
726 profiling of the adaptive response to mild decreases in oxygen concentration in the
727 roots of *Arabidopsis* plants. *Annals of Botany* **103**, 269–280.
728 Zhao F.J., Ma J.F., Meharg A.A. & McGrath S.P. (2009) Arsenic uptake and metabolism in
729 plants. *New Phytologist* **181**, 777-794.
730 Zhu Y-G., Williams P.N. & Meharg A.A. (2008) Exposure to inorganic arsenic from rice, A
731 global health issue? *Environmental Pollution* **154**, 169-171.
732 Zimmermann P., Hirsch-Hoffmann M., Hennig L. & Gruissem W. (2004)
733 GENEVESTIGATOR. *Arabidopsis* microarray database and analysis toolbox. *Plant*
734 *Physiology* **136**, 2621-2632**.**
735

FIGURE LEGENDS

Figure 1. As(V) sensitivity of root elongation in *mtlpd2* mutant seedlings. WT and mutant seedlings were grown for 5 d and exposed to 0 and 200 μM As(V). Ws and Col-0 are the WT accessions corresponding to *mtlpd2-1* and *mtlpd2-2*, respectively. (a), Phenotypes of seedlings after 3 d As(V) exposure. Bar = 1 cm. (b), Increase in root length during 3 d As(V) exposure. (c), The total number of branch roots after 4 d As(V) exposure. For (b) and (c), the values shown are means ± SE (n = 10 to 20 seedlings). Significant differences compared to WT are indicated; *P < 0.05 and **P < 0.01 (Student's t test).

Figure 2. Sensitivity of *mtlpd2* mutants to As(V). WT and mutant seedlings were grown for 5 d and exposed to 0 and 200 μM As(V). Ws and Col-0 are the WT accessions corresponding to *mtlpd2-1* and *mtlpd2-2*, respectively. (a) Fresh weight of seedlings after 10 d exposure to As(V). (b) Shoot anthocyanin accumulation after 15 d exposure to As(V). In (a) and (b), values are means ± SE (n = 4 replicates of 2 or 3 seedlings). Significant differences compared to WT are indicated; *P < 0.05 and **P < 0.01 (Student's t test).

Figure 3. *mtLPD2* promoter activity. Five-day old (a, b) and 12-d-old (c, d, e, f) seedlings containing *mtLPD2* promoter-GUS fusion constructs were stained for GUS activity. (a) Whole seedling. (b) Root tip. (c) Shoot. (d) Main root. (e) Established lateral root. (f) Newly initiated lateral root. Bar (a, c) = 500 μm. Bar (b, d, e, f) = 50 μm.

Figure 4. Arsenic accumulation in the *mtlpd2-2* mutant. WT and mutant seedlings were grown for 39 d before exposure to 0 and 50 μM As(V). Col-0 is the WT accession corresponding to *mtlpd2-2*. (a) Shoots and (b) roots of 42-d-old plants exposed to As(V) for the last 3 d of growth. Means ± SE (n = 4) are shown. Significant differences compared to WT are indicated; *P < 0.05 and **P < 0.01 (Student's t test).

764 **Figure 5.** Decreased mtLPD protein amount and activity in *mtlpd2-2* plants. Mitochondria
765 were isolated from 2-wk-old WT and *mtlpd2-2* plants. (a) Immunoblot of 50 µg
766 mitochondrial protein probed with an anti-pea LPD antiserum. (b) LPD activity was
767 measured in isolated mitochondria using NAD^+ and dihydrolipoic acid as substrates. (c), As
768 (b), except NADH and α-lipoic acid were the substrates. For (b) and (c), means ± SE (n = 3 to
769 5) are shown. Significant differences compared to WT are indicated; *P < 0.05 and **P <
770 0.01 (Student's t test).
771
772 **Figure 6.** The sensitivity of mtLPD activity from wild-type *Arabidopsis* to As(V) and As(III).
773 Mitochondria were isolated from 2-wk-old wild-type plants and mtLPD activity measured. (a)
774 The effect of As(III). (b) The effect of As(V). For (a) and (b) means ± SE (n = 3 or 4) are
775 shown. The SE for some data points was smaller than the size of the point.
776
777 **Figure 7.** As(III) sensitivity of the *mtlpd2-2* mutant. Mutant and corresponding Col-0 WT
778 seedlings were grown for 4 d and exposed to As(III). (a) Increase in root length after 4 d
779 exposure to As(III). Means ± SE (n = 10 to 15) are shown. (b) Fresh weight per plant after 10
780 d exposure to As(III). Means ± SE (n = 4 plates; 2 to 4 seedlings from each plate were pooled
781 and treated as one biological replicate) are shown. For (a) and (b) significant differences
782 compared to WT are indicated; *P < 0.05 and **P < 0.01 (Student's t test).
783
784 **Figure 8.** Metabolite changes induced by As(V) in *Arabidopsis* roots.
785 Six-day-old *mtlpd2-2* and the corresponding Col-0 WT seedlings were grown in the presence
786 or absence of 200 µM As(V) for a further 9 days. Metabolites were detected in roots by
787 GC-MS. The main links among the detected metabolites (black) and undetected landmark
788 metabolites (gray) are shown (arrows), as are the positions of the steps catalysed by PDC (1),
789 OGDC (2), GDC (3) and BCOADC (4). Malonate inhibits succinate dehydrogenase (square
790 arrow). The ratios of the metabolites in the comparisons of *mtlpd2* to WT (left-hand box),
791 WT + As(V) to WT (center box) and *mtlpd2* + As(V) to *mtlpd2* (right-hand box) are shown in

792 the boxes near each label. Colors represent ≥2, ≥5, ≥10 and ≥20-fold higher (red colors) or
793 lower (blue colors) metabolite levels in the treated sample compared to the untreated sample.
794 Some metabolites were not detected in both samples being compared (black fill). Significant
795 differences (•) of at least 2-fold were determined by a t-test (P<0.05, n =4 or 6).
796 Abbreviations: 2OG, 2-oxoglutarate; 3-PG, 3-phosphoglycerate; Ac-CoA, acetyl-CoA; Asc,
797 ascorbate; Ala, alanine; Arg, arginine; Asn, asparagine; Asp, aspartate; β-Ala, *beta*-alanine;
798 Cit, citrate; Cys, cysteine; E4P, erythrose-4-phosphate; Erol, *meso*-erythritol; FA, fatty acids;
799 Fru, fructose; Fum, fumarate; G6P, glucose-6-phosphate; GABA, *gamma*-aminobutyrate; Gct,
800 glycerate; Gcl, glycolate; Gen, gentiobiose; Glc, glucose; Gln, glutamine; Glu, glutamate;
801 Gly, glycine; Glol, galactanol; Grt, glucarate; Gxl, glyoxylate; hSer, homoserine; Ile,
802 isoleucine; Ino, *myo*-inositol; Leu, leucine; Lys, lysine; Mal, malate; Man, mannose; Mel,
803 melibiose; Mln, malonate; Phe, phenylalanine; Pro, proline; Pyr, pyruvate; Raf, raffinose;
804 RUBP, ribulose-1,6-bisphosphate; Ser, serine; Stig, stigmasterol; Succ, succinate; Tre,
805 trehalose; Thr, threonine; Trn, threonate; Trp, tryptophan; toco, alpha-tocopherol; Tyr,
806 tyrosine; Val, valine.
807
808
809
810 **SUPPORTING INFORMATION**
811 The following supplementary material is available for this article online:
812 **Figure S1.** Molecular characterization of *mtLPD2* T-DNA insertion mutants.
813 **Figure S2.** Complementation of *mtlpd2* mutant.
814 **Figure S3.** The response of *mtlpd2* mutants to As(V).
815 **Figure S4.** E2 subunit abundance is unchanged in *mtlpd2-2*.
816 **Table S1.** Oligonucleotide primers used in this study.
817 **Table S2.** Ratios of metabolites compared to the WT tissue in the absence of arsenate [As(V)]

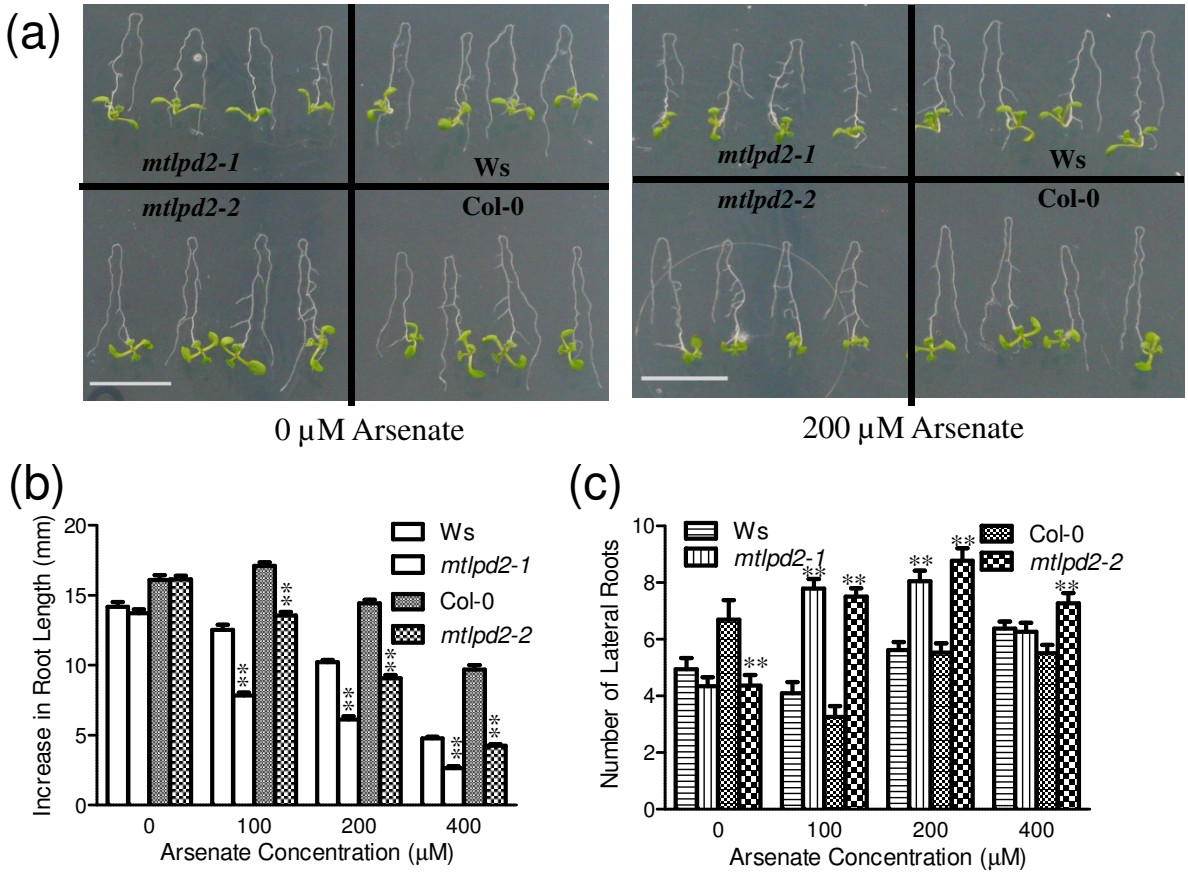
(a)
mtlpd2-1
Ws
mtlpd2-2
Col-0
0 µM Arsenate
mtlpd2-1
Ws
mtlpd2-2
Col-0
200 µM Arsenate
(b)
Increase in Root Length (mm)
Ws
mtlpd2-1
Col-0
mtlpd2-2
Arsenate Concentration (µM)
(c)
Number of Lateral Roots
Ws
mtlpd2-1
Col-0
mtlpd2-2
Arsenate Concentration (µM)

Figure 1.

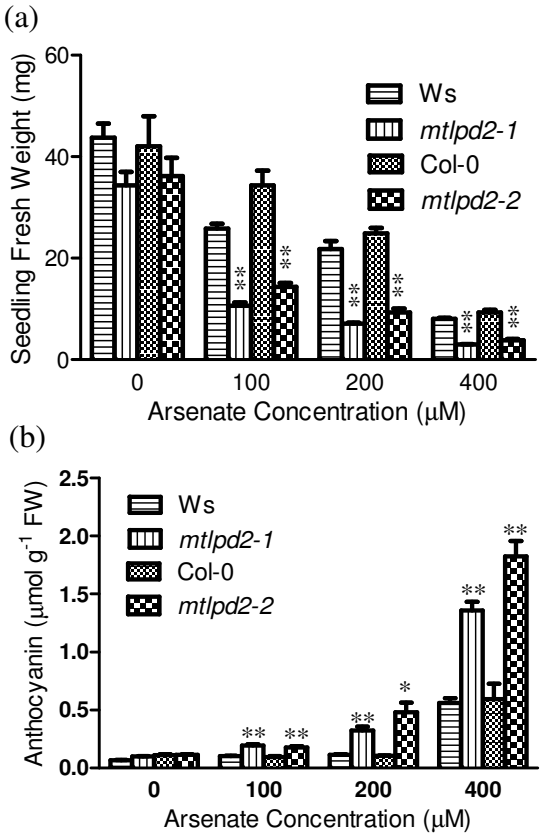
(a)
Seedling Fresh Weight (mg)
60
40
20
0
Ws
mtlpd2-1
Col-0
mtlpd2-2
0
100
200
400
Arsenate Concentration (μM)
(b)
Anthocyanin (μmol g-1 FW)
2.5
2.0
1.5
1.0
0.5
0.0
Ws
mtlpd2-1
Col-0
mtlpd2-2
0
100
200
400
Arsenate Concentration (μM)

Figure 2

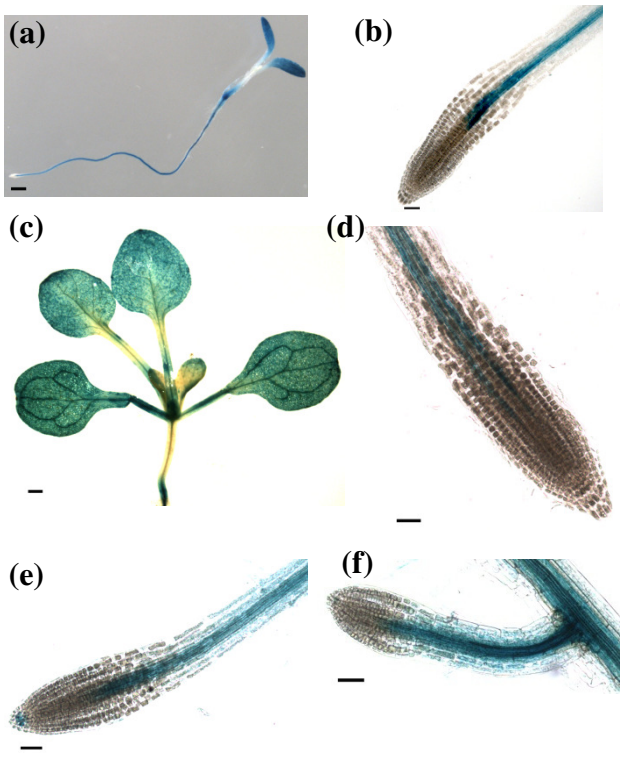

Figure 3.

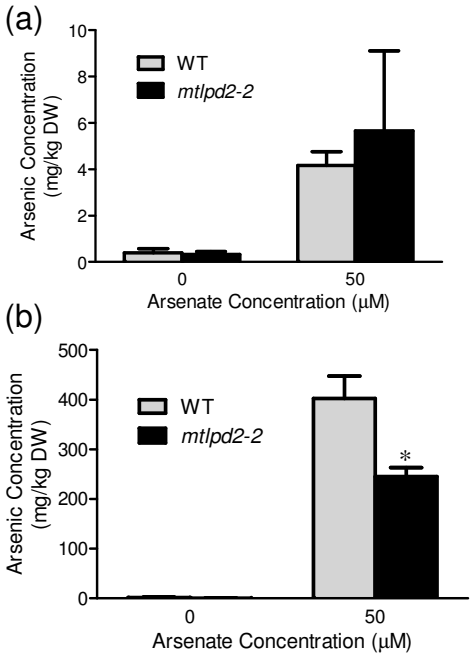
(a)
Arsenic Concentration (mg/kg DW)
10
8
6
4
2
0
WT
mtlpd2-2
0
50
Arsenate Concentration (μM)
(b)
Arsenic Concentration (mg/kg DW)
500
400
300
200
100
0
WT
mtlpd2-2
*
0
50
Arsenate Concentration (μM)

Figure 4.

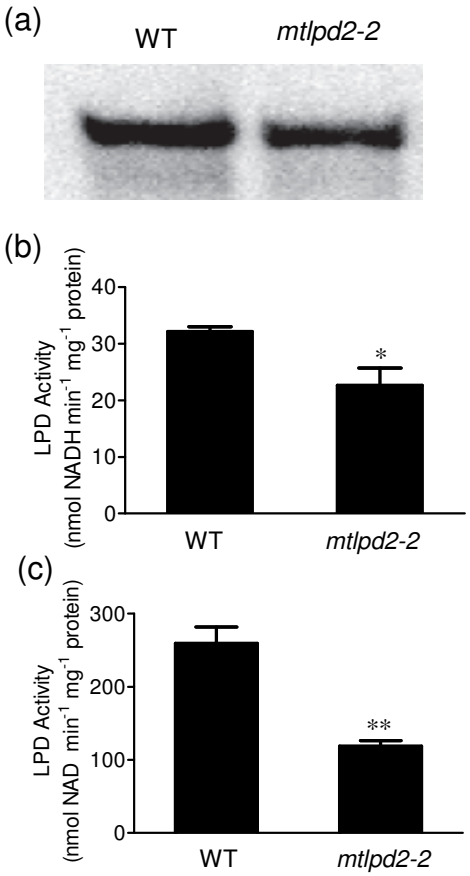
(a)
WT
mtlpd2-2
(b)
LPD Activity
(nmol NADH min-1 mg-1 protein)
40
30
20
10
0
*
WT
mtlpd2-2
(c)
LPD Activity
(nmol NAD min-1 mg-1 protein)
300
200
100
0
**
WT
mtlpd2-2

Figure 5.

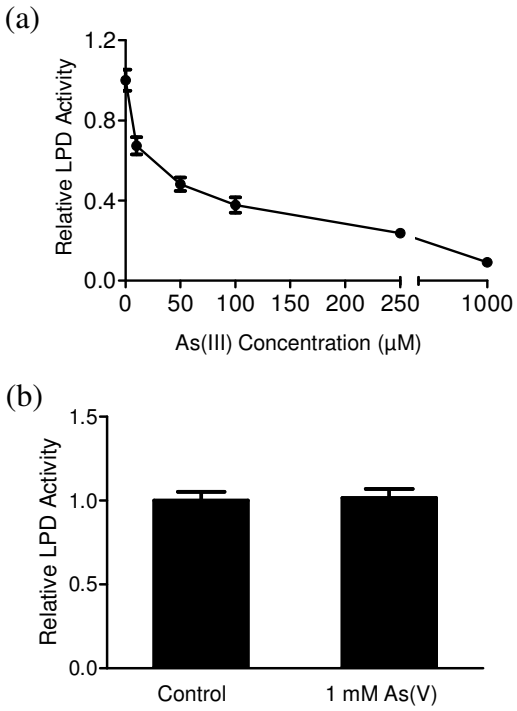
(a)
1.2
0.8
0.4
0.0
Relative LPD Activity
0
50
100
150
200
250
1000
As(III) Concentration (μM)
(b)
1.5
1.0
0.5
0.0
Relative LPD Activity
Control
1 mM As(V)

Figure 6.

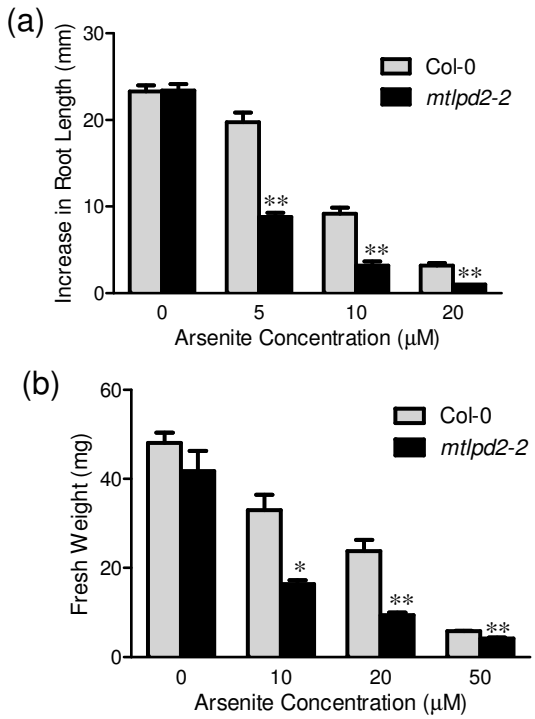
(a)
Increase in Root Length (mm)
30
20
10
0
Col-0
mtlpd2-2
**
**
**
0
5
10
20
Arsenite Concentration (μM)
(b)
Fresh Weight (mg)
60
40
20
0
Col-0
mtlpd2-2
*
**
**
0
10
20
50
Arsenite Concentration (μM)

Figure 7.

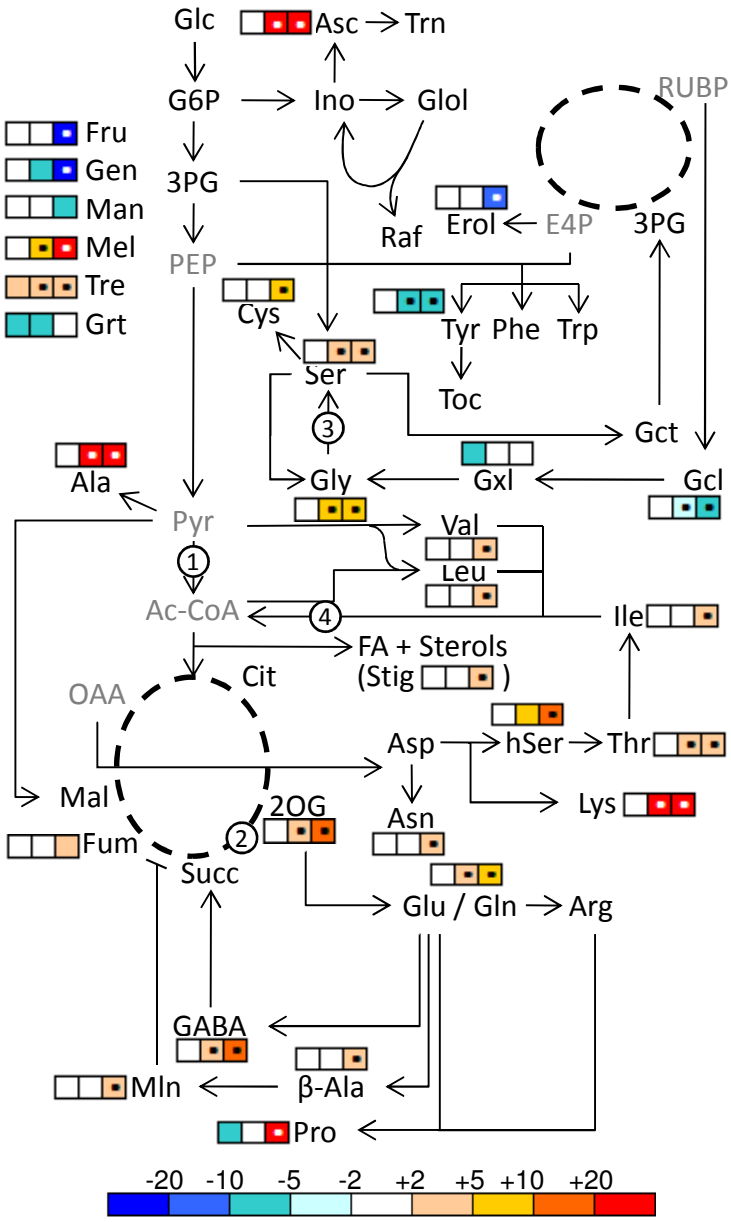
Glc
Asc
Trn
G6P
Ino
Glol
RUBP
Fru
Gen
Man
Mel
Tre
Grt
3PG
Raf
Erol
E4P
3PG
PEP
Cys
Tyr
Phe
Trp
Ser
Toc
3
Gct
Ala
Gly
Gxl
Gcl
Pyr
Val
1
Leu
Ac-CoA
4
Ile
FA + Sterols
(Stig)
Cit
OAA
Asp
hSer
Thr
Mal
2OG
Asn
Lys
Fum
2
Succ
Glu / Gln
Arg
GABA
Mln
β-Ala
Pro
-20
-10
-5
-2
+2
+5
+10
+20

Figure 8.

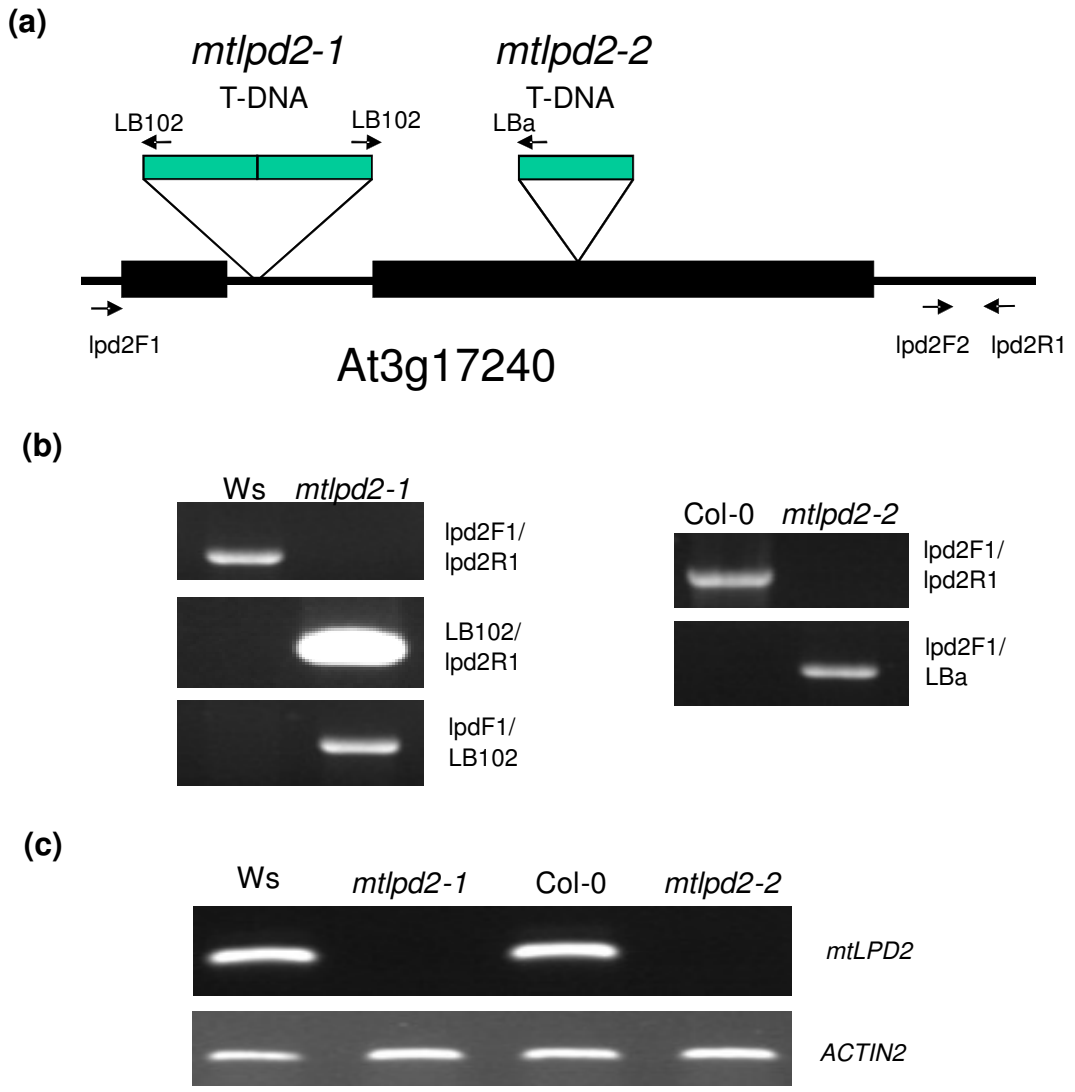

Figure S1. Molecular characterization of *mtLPD2* T-DNA insertion mutants.

(a) Schematic representation of the *mtLPD2* (At3g17240) genomic DNA region. Black boxes indicate exons, while black lines indicate introns and untranslated regions (UTR). The sizes of T-DNAs are not to scale. The locations of primers used for PCR genotyping and RT-PCR are shown (arrows).

(b) Identification of the T-DNA insertion site in the mtlpd2 alleles. Genomic DNA from mtlpd2-1 and mtlpd2-2 mutant plants as well as their corresponding wild-types Wassilewskija (Ws) and Columbia (Col-0) respectively were isolated and amplified by PCR using the primer combinations indicated on the right of each figure.

(c) Semi-quantitative RT-PCR analysis of the mtLPD2 T-DNA insertion lines using RNA isolated from whole wild-type and mutant seedlings. At3g18780 (ACTIN2) was used as amplification control.

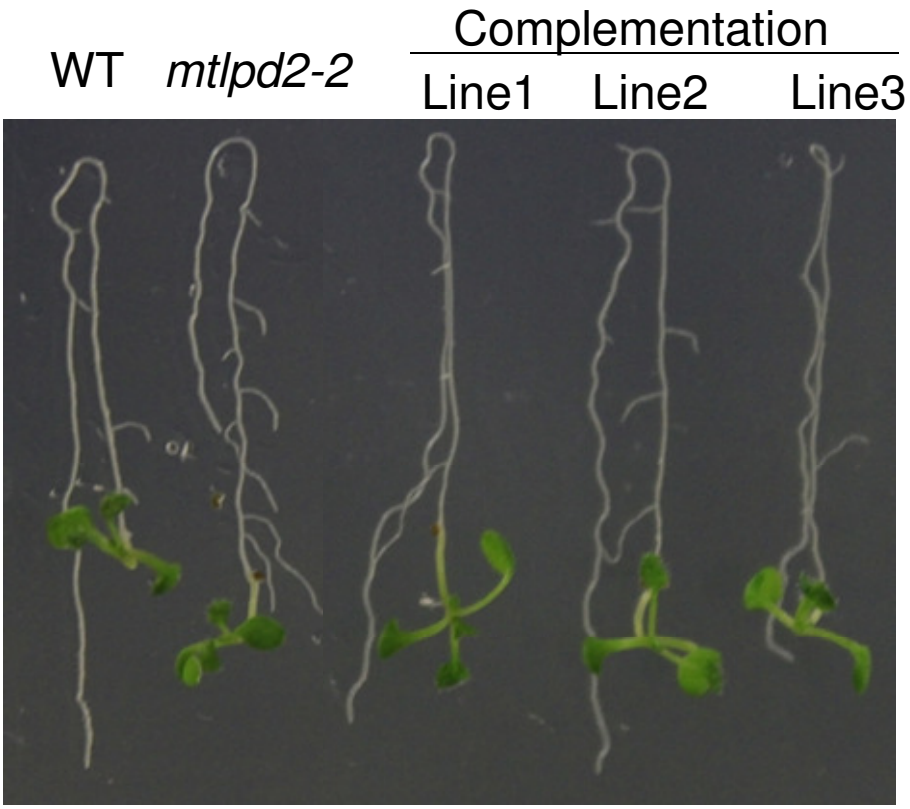

Figure S2. Complementation of *mtlpd2* mutant.
The *mtlpd2-2* mutant was complemented with a genomic DNA fragment containing the *mtLPD2* gene. Typical complemented T2 seedlings grown 5 d before exposure to 200 µM As(V) for a further 5 d are shown.

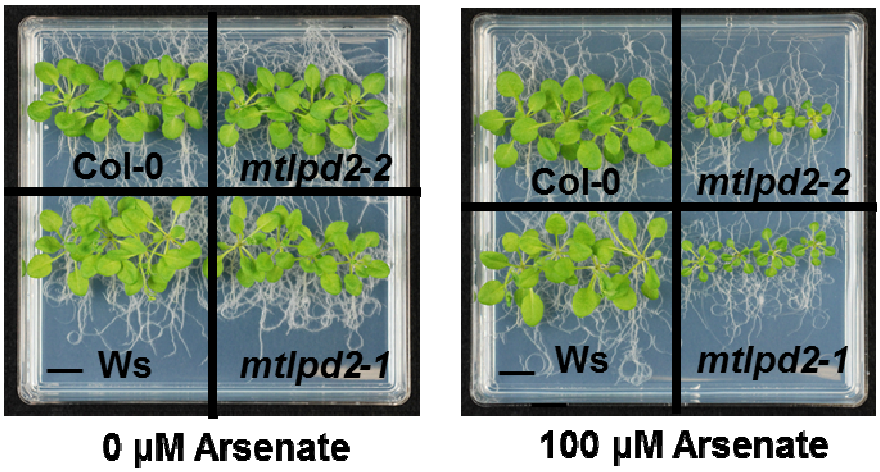

Figure S3. The response of *mtlpd2* mutants to As(V).
mtlpd2 mutant and corresponding wild-type seedlings grown on media with and without As(V). Plants were grown for four days with plates in a vertical position followed by ten days in a horizontal position.

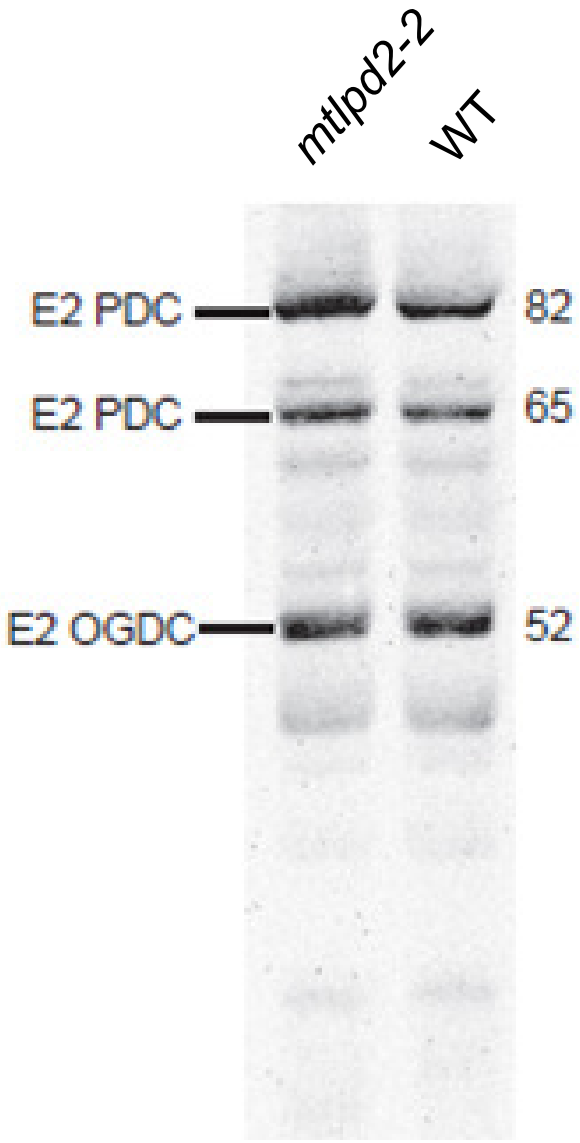

Figure S4. E2 subunit abundance is unchanged in *mtlpd2-2*.
Total mitochondrial protein (50 µg) from wild-type and *mtlpd2-2* mutant seedlings were immunoblotted and probed with polyclonal anti-liopic acid antibodies.

Table S1. Primer sequences used

Primer Name	Sequences
LPD2F1	GCCAAAGTCTCTCTTCTCCATC
lpd2R1	CACCGATCATACCTGATTAATCAC
LB102A	GATGCACTCGAAATCAGCCAATTTTAGAC
LBa1	TGGTTCACGTAGTGGGCCATCG
primers	GGGGACAAGTTTGTACAAAAAAGCAGGCTTGCCAAACATGGCTG
chen45F	CTTTACAC
chen45R	GGGGACCACTTTGTACAAGAAAGCTGGGTCCGTTATTGTTGTTGT TGTTGTTG

Supplemental Methods

Gateway™ technology (Invitrogen) was used to generate vector for plant transformation. A 4.5 kb fragment containing the 2.2-kb promoter fragment plus the *mtLPD2* coding region and 3'UTR (primers chen45F, GGGGACAAGTTTGTACAAAAAAGCAGGCTTGCCAAACATGGCTGCTTTACAC and chen46R, GGGGACCACTTTGTACAAGAAAGCTGGGTCACTGAACACAATCATACAGTG) was amplified from *Arabidopsis* genomic DNA. This PCR product was moved into pDONR221 (Invitrogen) followed by sequencing to confirm the sequences before transferring into the plant expression vector pMDC99 (Curtis and Grossniklaus, 2003) to generate pMDC99:mtLPD2. This vector was introduced into *Agrobacterium tumefaciens* strain GV3101 via electroporation. pMDC99:mtLPD2 was introduced into *mtlpd2-2* plants by the floral dip method (Clough and Bent, 1998). Transformed seeds were selected on solid MS medium (Phytotechnology Laboratories) containing 20 $\mu g\ mL^{-1}$ hygromycin.

Supplemental References

Clough S.J., Bent A.F. (1998). *Floral dip: A simplified method for Agrobacterium-mediated transformation of Arabidopsis thaliana. Plant J. 16: 735–743.*

Curtis M.D., Grossniklaus U. (2003). A gateway cloning vector set for high-throughput functional analysis of genes in planta. *Plant Physiol.* **133,** 462-469.

Table S2. Ratios of metabolites compared to the analogous WT tissue in the absence of arsenate [As(V)]. WT and *mtlpd2* seedlings were grown in the presence or absence of 200 µM As(V). Metabolite levels were determined by GC-MS and normalised to the relative signals from the same tissue of WT control seedlings not exposed to arsenate [0 As(V)].
Values shown are means ± SD (n = 5 or 6). Significance of differences compared to the ratio of 0 As(V) WT / 0 As(V) WT was determined by a t-test (n = 5 or 6)

P < 0.05 P < 0.01 ND = metabolite not detected in either sample
Ratios where a metabolite was not detected in one sample are shown in green color. In these cases, a value of 0.01, the minimum signal detected, was assigned to allow ratios to be calculated
The data shown in italics have less reliability, as no more than 50 % of the replicates gave a signal, such that n= 1 to 3.

Metabolite		Root				Shoot			
		WT / 0 As(V) WT		mtlpd2 / 0 As(V) WT		WT / 0 As(V) WT		mtlpd2 / 0 As(V) WT	
		0 As(V)	200 µM As(V)	0 As(V)	200 µM As(V)	0 As(V)	200 µM As(V)	0 As(V)	200 µM As(V)
Organic acidS	(iso)citrate	1.00 ± 0.07	0.90 ± 0.06	1.06 ± 0.09	0.97 ± 0.09	1.00 ± 0.27	0.78 ± 0.21	0.91 ± 0.10	0.70 ± 0.06
	ascorbate	ND	86.14 ± 6.54	ND	145.42 ± 17.05	1.00 ± 0.20	*0.16 ± 0.04*	0.11 ± 0.00	0.11 ± 0.00
	benzoate	1.00 ± 0.09	1.06 ± 0.08	1.13 ± 0.08	0.69 ± 0.03	*1.00 ± 0.23*	3.86 ± 0.34	0.77 ± 0.00	3.79 ± 0.40
	fumarate	1.00 ± 0.08	0.91 ± 0.11	1.03 ± 0.06	2.42 ± 0.59	1.00 ± 0.03	0.90 ± 0.08	0.90 ± 0.05	1.57 ± 0.28
	glucarate	*1.00 ± 0.34*	0.29 ± 0.00	*0.42 ± 0.13*	0.29 ± 0.00	ND	ND	*3.07 ± 1.31*	34.40 ± 2.78
	gluconate	1.00 ± 0.07	1.29 ± 0.06	1.11 ± 0.03	1.35 ± 0.10	1.00 ± 0.03	1.08 ± 0.18	1.09 ± 0.06	2.80 ± 0.30
	glycerate	1.00 ± 0.23	1.02 ± 0.14	1.19 ± 0.17	1.01 ± 0.09	1.00 ± 0.20	1.36 ± 0.08	1.71 ± 0.18	3.31 ± 0.20
	glycolate	1.00 ± 0.09	0.50 ± 0.05	1.08 ± 0.07	0.44 ± 0.10	1.00 ± 0.09	0.97 ± 0.06	1.03 ± 0.06	1.99 ± 0.10
	glyoxylate	*1.00 ± 0.41*	*0.67 ± 0.20*	*0.47 ± 0.07*	0.36 ± 0.00	1.00 ± 0.17	*0.25 ± 0.08*	0.45 ± 0.07	0.83 ± 0.06
	lactate	ND	ND	ND	ND	*1.00 ± 0.94*	*0.92 ± 0.86*	*3.11 ± 1.37*	*0.92 ± 0.85*
	malate	1.00 ± 0.08	0.80 ± 0.03	0.92 ± 0.08	0.96 ± 0.04	1.00 ± 0.12	0.81 ± 0.06	1.03 ± 0.06	1.05 ± 0.04
	maleate	ND	ND	ND	ND	1.00 ± 0.25	0.01 ± 0.00	0.65 ± 0.02	*0.33 ± 0.21*
	malonate	1.00 ± 0.06	1.49 ± 0.11	0.87 ± 0.07	1.81 ± 0.11	1.00 ± 0.10	0.98 ± 0.06	0.87 ± 0.03	1.63 ± 0.10
	nicotinic acid	1.00 ± 0.07	0.01 ± 0.00	1.19 ± 0.10	0.01 ± 0.00	1.00 ± 0.12	0.90 ± 0.09	0.99 ± 0.03	1.63 ± 0.09
	oxoglutarate, 2-	1.00 ± 0.06	3.08 ± 0.35	1.35 ± 0.11	25.60 ± 2.37	1.00 ± 0.06	0.99 ± 0.08	1.42 ± 0.06	1.02 ± 0.05
	phosphoglycerate, 3-	ND	ND	ND	ND	1.00 ± 0.29	0.84 ± 0.11	2.08 ± 0.28	2.59 ± 0.51
	p-hydroxybenzoate	*1.00 ± 0.29*	4.05 ± 1.02	0.71 ± 0.00	*3.16 ± 1.41*	ND	ND	ND	ND
	pyrrolecarboxylate, 2-	1.00 ± 0.07	1.37 ± 0.14	*0.84 ± 0.04*	*0.89 ± 0.09*	ND	ND	ND	ND
	sinapinate	*1.00 ± 0.03*	*1.00 ± 0.06*	0.97 ± 0.00	*1.25 ± 0.19*	1.00 ± 0.15	0.92 ± 0.09	0.98 ± 0.08	1.64 ± 0.18
	succinate	1.00 ± 0.07	1.10 ± 0.04	1.12 ± 0.06	1.14 ± 0.08	1.00 ± 0.13	0.94 ± 0.04	1.08 ± 0.06	1.43 ± 0.08
	threonate	1.00 ± 0.05	1.25 ± 0.05	1.19 ± 0.06	1.27 ± 0.04	1.00 ± 0.07	1.38 ± 0.06	1.11 ± 0.08	3.43 ± 0.27
Amino acids	alanine	*1.00 ± 0.67*	109.75 ± 16.28	*1.64 ± 1.03*	66.16 ± 6.85	1.00 ± 0.07	1.73 ± 0.36	*0.43 ± 0.28*	1.14 ± 0.10
	alanine, β-	1.00 ± 0.04	1.18 ± 0.19	0.84 ± 0.08	3.61 ± 0.29	1.00 ± 0.10	1.98 ± 0.34	0.83 ± 0.07	1.68 ± 0.12
	asparagine	1.00 ± 0.12	1.70 ± 0.13	0.97 ± 0.07	2.97 ± 0.11	1.00 ± 0.14	2.07 ± 0.33	1.23 ± 0.20	1.81 ± 0.16
	aspartate	1.00 ± 0.09	1.54 ± 0.10	0.87 ± 0.11	0.79 ± 0.08	1.00 ± 0.11	1.65 ± 0.13	1.55 ± 0.14	1.60 ± 0.19
	cysteine	1.00 ± 0.11	*0.68 ± 0.33*	*0.66 ± 0.22*	3.77 ± 0.19	ND	*1.17 ± 0.17*	ND	*1.75 ± 0.36*
	GABA	1.00 ± 0.19	3.09 ± 0.31	1.13 ± 0.11	11.39 ± 0.91	1.00 ± 0.42	1.46 ± 0.43	0.80 ± 0.13	3.67 ± 0.59
	glutamate / glutamine	1.00 ± 0.10	2.76 ± 0.17	1.16 ± 0.08	10.09 ± 0.59	1.00 ± 0.11	1.68 ± 0.23	1.31 ± 0.11	1.61 ± 0.23
	glycine	1.00 ± 0.14	6.48 ± 0.65	1.24 ± 0.05	8.51 ± 0.60	1.00 ± 0.39	5.63 ± 1.57	1.08 ± 0.28	7.81 ± 2.35
	homoserine	*1.00 ± 0.23*	5.64 ± 1.54	0.77 ± 0.00	14.16 ± 0.88	ND	ND	ND	ND
	isoleucine	1.00 ± 0.10	1.48 ± 0.04	1.15 ± 0.13	2.50 ± 0.14	ND	ND	ND	ND
	leucine	1.00 ± 0.05	1.68 ± 0.03	1.13 ± 0.07	3.15 ± 0.20	ND	ND	ND	ND
	lysine	ND	151.59 ± 3.90	ND	336.76 ± 18.19	ND	ND	ND	ND
	phenylalanine	1.00 ± 0.14	1.15 ± 0.05	1.04 ± 0.06	1.21 ± 0.05	*1.00 ± 0.35*	*2.61 ± 0.97*	*1.25 ± 0.60*	*1.24 ± 0.59*
	proline	1.00 ± 0.10	1.91 ± 0.10	0.32 ± 0.22	6.54 ± 0.62	1.00 ± 0.09	0.97 ± 0.22	0.81 ± 0.11	3.00 ± 0.52
	pyroglutamate	1.00 ± 0.07	1.87 ± 0.14	1.15 ± 0.06	1.65 ± 0.62	1.00 ± 0.06	1.11 ± 0.09	1.06 ± 0.07	1.47 ± 0.04
	serine	1.00 ± 0.09	3.68 ± 0.26	1.26 ± 0.06	3.26 ± 0.17	1.00 ± 0.10	1.17 ± 0.13	1.15 ± 0.08	0.98 ± 0.08
	threonine	1.00 ± 0.08	3.07 ± 0.21	1.25 ± 0.05	2.95 ± 0.13	1.00 ± 0.09	1.11 ± 0.12	1.15 ± 0.07	0.92 ± 0.07
	tyrosine	1.00 ± 0.15	*0.23 ± 0.17*	1.27 ± 0.13	0.06 ± 0.00	ND	ND	*1.17 ± 0.17*	*1.95 ± 0.75*
	valine	1.00 ± 0.05	1.91 ± 0.08	1.18 ± 0.04	2.71 ± 0.10	1.00 ± 0.12	1.27 ± 0.23	1.28 ± 0.05	1.38 ± 0.08
Carbohydrates	arabino-Hexos-2-ulose, bis(	1.00 ± 0.05	1.37 ± 0.04	1.07 ± 0.04	1.04 ± 0.03	1.00 ± 0.08	1.07 ± 0.07	1.06 ± 0.06	2.16 ± 0.14
	fructose	1.00 ± 0.03	0.74 ± 0.07	1.04 ± 0.04	0.02 ± 0.00	1.00 ± 0.09	0.65 ± 0.06	0.98 ± 0.06	2.01 ± 0.18
	fructose-6-phosphate	1.00 ± 0.08	0.85 ± 0.08	1.14 ± 0.03	0.89 ± 0.06	*1.00 ± 0.82*	*1.03 ± 0.86*	*3.15 ± 1.37*	*1.32 ± 1.15*
	gentiobiose	1.00 ± 0.16	*0.28 ± 0.22*	1.15 ± 0.15	0.05 ± 0.00	1.00 ± 0.14	0.66 ± 0.04	0.92 ± 0.03	1.02 ± 0.10
	glucose	1.00 ± 0.07	0.94 ± 0.11	1.18 ± 0.08	0.93 ± 0.08	1.00 ± 0.24	1.38 ± 0.26	0.50 ± 0.14	4.04 ± 0.40
	glucose-6-phosphate	1.00 ± 0.05	0.83 ± 0.12	1.11 ± 0.02	0.76 ± 0.09	1.00 ± 0.08	0.94 ± 0.09	1.43 ± 0.14	1.75 ± 0.10
	glycero-gulo-heptose O-me	1.00 ± 0.03	0.70 ± 0.07	1.15 ± 0.07	0.66 ± 0.06	1.00 ± 0.08	1.09 ± 0.06	1.32 ± 0.13	2.07 ± 0.25
	mannose	1.00 ± 0.16	0.57 ± 0.23	1.02 ± 0.39	0.33 ± 0.06	1.00 ± 0.09	1.13 ± 0.11	1.11 ± 0.17	1.86 ± 0.15
	melibiose	*1.00 ± 0.21*	5.21 ± 0.50	0.79 ± 0.00	19.82 ± 4.85	1.00 ± 0.14	4.10 ± 0.53	0.53 ± 0.06	7.34 ± 0.61
	raffinose	ND	ND	ND	ND	1.00 ± 0.28	1.84 ± 0.30	1.85 ± 0.12	3.07 ± 0.37
	trehalose	1.00 ± 0.05	2.61 ± 0.46	2.97 ± 1.83	14.01 ± 2.24	ND	*9.86 ± 5.61*	*6.26 ± 5.26*	79.19 ± 12.60
Sugar alcohols	galactinol	1.00 ± 0.07	0.73 ± 0.04	1.10 ± 0.04	0.87 ± 0.09	1.00 ± 0.06	1.07 ± 0.03	1.28 ± 0.07	1.89 ± 0.23
	meso-erythritol	1.00 ± 0.19	0.06 ± 0.01	0.69 ± 0.21	0.09 ± 0.01	0.83 ± 0.30	22.58 ± 14.38	0.93 ± 0.14	1.79 ± 0.26
	myo-inositol	1.00 ± 0.04	1.11 ± 0.06	1.04 ± 0.04	1.34 ± 0.05	1.00 ± 0.07	0.80 ± 0.05	0.91 ± 0.05	1.18 ± 0.09
	phytol	ND	ND	ND	ND	1.00 ± 0.13	0.69 ± 0.10	1.58 ± 0.36	1.56 ± 0.27
Fatty acids	linolenate	ND	ND	ND	ND	1.00 ± 0.09	0.66 ± 0.10	1.00 ± 0.08	0.70 ± 0.08
	palmitate	1.00 ± 0.12	1.09 ± 0.07	0.75 ± 0.14	1.01 ± 0.05	1.00 ± 0.12	0.72 ± 0.12	0.68 ± 0.06	0.57 ± 0.12
	stearate	1.00 ± 0.10	0.98 ± 0.09	0.90 ± 0.07	1.09 ± 0.07	1.00 ± 0.10	1.06 ± 0.07	0.85 ± 0.06	0.80 ± 0.03
Sterols	campesterol	1.00 ± 0.03	0.97 ± 0.05	1.08 ± 0.04	1.06 ± 0.04	1.00 ± 0.08	0.99 ± 0.05	1.05 ± 0.03	1.16 ± 0.03
	sitosterol	1.00 ± 0.03	1.05 ± 0.05	1.21 ± 0.04	0.92 ± 0.03	1.00 ± 0.07	0.97 ± 0.05	1.02 ± 0.03	1.11 ± 0.02
	stigmasterol	1.00 ± 0.03	1.35 ± 0.07	1.14 ± 0.04	2.68 ± 0.10	ND	ND	ND	ND
other	allantoin derivative	1.00 ± 0.10	*0.29 ± 0.11*	*0.34 ± 0.14*	1.39 ± 0.20	ND	ND	ND	ND
	dihydroxydihydrofuran	*1.00 ± 0.60*	0.16 ± 0.00	0.16 ± 0.00	0.16 ± 0.00	1.00 ± 0.03	1.01 ± 0.13	0.96 ± 0.07	1.32 ± 0.09
	ethanolamine	1.00 ± 0.03	1.12 ± 0.08	1.21 ± 0.04	1.36 ± 0.07	1.00 ± 0.08	1.01 ± 0.12	1.42 ± 0.19	1.32 ± 0.06
	xylonic acid lacton	1.00 ± 0.08	1.27 ± 0.05	1.10 ± 0.03	0.92 ± 0.05	1.00 ± 0.07	0.86 ± 0.14	1.52 ± 0.15	3.60 ± 0.31
	α-tocopherol	ND	ND	ND	ND	1.00 ± 0.17	1.28 ± 0.24	1.45 ± 0.18	3.78 ± 0.39